

## Research Article

# A Human iPSC-Based *In Vitro* Neural Network Formation Assay to Investigate Neurodevelopmental Toxicity of Pesticides

Kristina Bartmann<sup>1,2</sup>, Farina Bendt<sup>1</sup>, Arif Dönmez<sup>1,2</sup>, Daniel Haag<sup>3</sup>, H. Eike Kefel<sup>1</sup>, Stefan Masjosthusmann<sup>1</sup>, Christopher Noel<sup>3</sup>, Ji Wu<sup>3</sup>, Peng Zhou<sup>3</sup> and Ellen Fritzsche<sup>1,2,4</sup>

<sup>1</sup>IUF – Leibniz Research Institute for Environmental Medicine, Duesseldorf, Germany; <sup>2</sup>DNTOX GmbH, Duesseldorf, Germany; <sup>3</sup>NeuCyte Inc., Mountain View, CA, USA; <sup>4</sup>Medical Faculty, Heinrich-Heine-University, Duesseldorf, Germany

### Abstract

Proper brain development is based on the orchestration of key neurodevelopmental processes (KNDP), including the formation and function of neural networks. If at least one KNDP is affected by a chemical, an adverse outcome is expected. To enable a higher testing throughput than the guideline animal experiments, a developmental neurotoxicity (DNT) *in vitro* testing battery (DNT IVB) comprising a variety of assays that model several KNDPs was set up. Gap analysis revealed the need for a human-based assay to assess neural network formation and function (NNF). Therefore, we established the human NNF (hNNF) assay. A co-culture comprised of human induced pluripotent stem cell (hiPSC)-derived excitatory and inhibitory neurons as well as primary human astroglia was differentiated for 35 days on microelectrode arrays (MEA), and spontaneous electrical activity, together with cytotoxicity, was assessed on a weekly basis after washout of the compounds 24 h prior to measurements. In addition to the characterization of the test system, the assay was challenged with 28 compounds, mainly pesticides, identifying their DNT potential by evaluation of specific spike-, burst-, and network parameters. This approach confirmed the suitability of the assay for screening environmental chemicals. Comparison of benchmark concentrations (BMC) with an NNF *in vitro* assay (rNNF) based on primary rat cortical cells revealed differences in sensitivity. Together with the successful implementation of hNNF data into a postulated stressor-specific adverse outcome pathway (AOP) network associated with a plausible molecular initiating event for deltamethrin, this study suggests the hNNF assay as a useful complement to the DNT IVB.

### 1 Introduction

The developing central nervous system is known to be more sensitive to exposure to toxic agents than the adult equivalent (Rodier, 1995). There is evidence that environmental chemicals contribute to neurodevelopmental disorders in children such as autism spectrum disorder, mental retardation, and cerebral palsy (NRC, 2000; Grandjean and Landrigan, 2006; Kuehn, 2010; Sagiv et al., 2010; Bennett et al., 2016).

Pesticides belong to one compound class that is demonstrably associated with causing developmental neurotoxicity (DNT) (Björpling-Poulsen et al., 2008). Today, only 35 of the 485 pesticides currently approved in the EU have been tested in DNT studies (Ockleford et al., 2018). The reason for this lack of testing, which generally applies to all chemicals (Goldman and Koduru,

2000; Crofton et al., 2012), lies in the current DNT *in vivo* testing guidelines, i.e., the OECD 426 (OECD, 2007) and EPA 870.6300 (U.S. EPA, 1998) guidelines. Their high resource intensity regarding time, money, and animals is a reason for the limited throughput of these studies (Smirnova et al., 2014). Furthermore, high variability and low reproducibility of *in vivo* experiments, as well as species differences, increase the uncertainty of *in vivo* guideline studies for DNT testing (Tsuji and Crofton, 2012; Terron and Bennekou, 2018; Sachana et al., 2019; Paparella et al., 2020).

In the last years, scientists from academia, industry, and regulatory authorities across the world agreed on the need for a standardized *in vitro* testing strategy, aiming for cheaper and faster generation of additional data for DNT hazard assessment (EFSA, 2013; Crofton et al., 2014; Bal-Price et al., 2015, 2018; Fritzsche et al., 2017, 2018a,b). Following this consensus, a DNT *in vitro* battery

Received June 3, 2022; Accepted April 24, 2023;  
Epub May 3, 2023; © The Authors, 2023.

ALTEX 40(3), 452-470. doi:10.14573/altex.2206031

Correspondence: Ellen Fritzsche, PhD  
IUF-Leibniz Research Institute for Environmental Medicine  
Auf'm Hennekamp 50  
40225 Duesseldorf, Germany  
(ellen.fritzsche@iuf-duesseldorf.de)

This is an Open Access article distributed under the terms of the Creative Commons Attribution 4.0 International license (<http://creativecommons.org/licenses/by/4.0/>), which permits unrestricted use, distribution and reproduction in any medium, provided the original work is appropriately cited.

(IVB) was compiled, which includes various DNT test methods covering different neurodevelopmental processes, so-called key events (KEs), and developmental stages to approximate the complexity of human brain development (Fritzsche, 2017; Fritzsche et al., 2017; Bal-Price et al., 2018). Within this DNT IVB, neurodevelopment is described by *in vitro* assays covering the following KEs: human neural progenitor cell (hNPC) proliferation (Baumann et al., 2014, 2015; Harrill et al., 2018; Nimtz et al., 2019; Masjosthusmann et al., 2020; Koch et al., 2022) and apoptosis (Druwe et al., 2015; Harrill et al., 2018), cell migration (Baumann et al., 2015, 2016; Nyffeler et al., 2017; Schmuck et al., 2017; Masjosthusmann et al., 2020; Koch et al., 2022), hNPC-neuronal (Baumann et al., 2015; Schmuck et al., 2017; Masjosthusmann et al., 2020; Koch et al., 2022) and oligodendrocyte differentiation (Fritzsche et al., 2015; Dach et al., 2017; Schmuck et al., 2017; Masjosthusmann et al., 2020; Klose et al., 2021; Koch et al., 2022), neurite outgrowth (*human*: Harrill et al., 2010, 2018; Krug et al., 2013; Hoelting et al., 2016; Masjosthusmann et al., 2020; Koch et al., 2022; *rat*: Harrill et al., 2013, 2018) as well as neuronal maturation and synaptogenesis (*rat*: Harrill et al., 2011, 2018).

Another crucial key neurodevelopmental process represented within the DNT IVB is the formation and function of neural networks, since nervous system development requires functional networks consisting of different types of neurons and glial cells (Brown et al., 2016; Frank et al., 2017; Shafer, 2019). Furthermore, certain brain disorders, like autism spectrum disorder, Alzheimer's and Parkinson's disease, are associated with dysfunctional neural synchronization (Uhlhaas and Singer, 2006). Important tools to study electrophysiology of such neural networks are microelectrode arrays (MEA), which record extracellular local field potentials on multiple electrodes at different locations of the network and provide information on electrical activity, firing patterns, and synchronicity of the neural networks (Johnstone et al., 2010). So far, DNT *in vitro* testing for synaptogenesis and neuronal activity is mainly performed in assays based on rat primary cortical cells (Brown et al., 2016; Frank et al., 2017). The use of a human cell model to assess this endpoint has been identified as a gap in the current DNT IVB because the potential for species-specific features is still unknown (Crofton and Mundy, 2021).

The introduction of human induced pluripotent stem cells (hiPSC) (Takahashi et al., 2007) has extensively advanced the field of biomedical sciences including testing for DNT. It has been shown that hiPSC-derived neural networks growing directly on MEAs exhibit spontaneous neuronal activity with organized spiking and bursting patterns (Odawara et al., 2016; Ishii et al., 2017; Nimtz et al., 2020; Tukker et al., 2020a; Bartmann et al., 2021), which can be modulated with known neurotoxicants and

drugs (Odawara et al., 2018; Nimtz et al., 2020; Tukker et al., 2020b). The neural induction of hiPSCs towards functional neuronal cultures comes with many advantages, especially with regard to disease modelling, but bears the issue of high variability between batches and cell lines. This variability is mostly due to the fact that every neural network differentiates into a variable number of neuronal subtypes. In addition, the generation of sufficiently active networks takes weeks to months (Hofrichter et al., 2017; Hyvärinen et al., 2019). The use of commercially available hiPSC-derived neurons with quality- and cell ratio-controlled, reproducible cells provided in large quantities circumvents these problems (Little et al., 2019).

In this study we present the establishment of a human neural network formation (hNNF) assay based on a commercially available kit, which consists of hiPSC-derived excitatory and inhibitory neurons and primary astroglia (SynFire, NeuCyte, USA). Pharmacological modulation confirmed the functionality of both neuronal subtypes, and chronic treatment over 35 days revealed the ability of the cell model to detect alterations by bisindolylmaleimide I (Bis-I) via a known mode of action (MoA). The assay was challenged with a test set of 28 substances and displayed compound-specific effects on network development.

## 2 Materials and methods

### Compounds

In the present study, 28 substances with different concerns regarding their DNT potential were tested. The compounds are part of a training set used for the current DNT *in vitro* battery (Blum et al., 2022; Carstens et al., 2022). More information on compound selection can be found in Masjosthusmann et al. (2020). As an assay negative control, acetaminophen was included in the test set. The protein kinase C (PKC) inhibitor Bis-I was used as an assay positive control, together with bicuculline (BIC) and cyanquinaline (6-cyano-7-nitroquinoxaline-2,3-dione; CNQX) for acute pharmacological treatment of networks. Bis-I is known to decrease neurite outgrowth and firing/bursting rates of rat neural networks (Harrill et al., 2011; Robinette et al., 2011), whereas BIC and CNQX are GABAergic and glutamatergic receptor inhibitors, respectively. Compounds were dissolved in dimethyl sulfoxide (DMSO) or water to a stock concentration of 20 mM with exception of rotenone (100 mM), BIC (15 mM), and CNQX (30 mM). Applied concentrations ranged from 0.027 to 20 µM and 0.0004 to 0.3 µM for rotenone. Bis-I was applied at 5 µM, BIC at 3 µM, and CNQX at 30 µM. CAS registry numbers, suppliers, and further information are collected in Table S1<sup>1</sup>.

<sup>1</sup> doi:10.14573/altex.2206031s1

### Abbreviations

AOP, adverse outcome pathway; AUC, area under the curve; AUNCC, area under normalized cross-correlation; BIC, bicuculline; Bis-I, bisindolylmaleimide I; BMC, benchmark concentration; BMR, benchmark response; CI, confidence interval; COV, coefficient of variation; CNQX, cyanquinaline; DIV, days *in vitro*; DMSO, dimethyl sulfoxide; DNT, developmental neurotoxicity; excitatory:inhibitory (ex:inh); FBS, fetal bovine serum; FPKM, fragments per kilobase per million; hiPSC, human induced pluripotent stem cells; IN, induced neuronal cells; IN:glia, induced neuronal and glial cells; MSE, most sensitive endpoint; LG, ligand-gated; MIE, molecular initiating event; NPC, neural progenitor cell; IVB, *in vitro* battery; KE, key event; KNDP, key neurodevelopmental process; MEA, microelectrode array; MoA, mode of action; NNF, neural network formation and function; PKC, protein kinase C; VG, voltage-gated

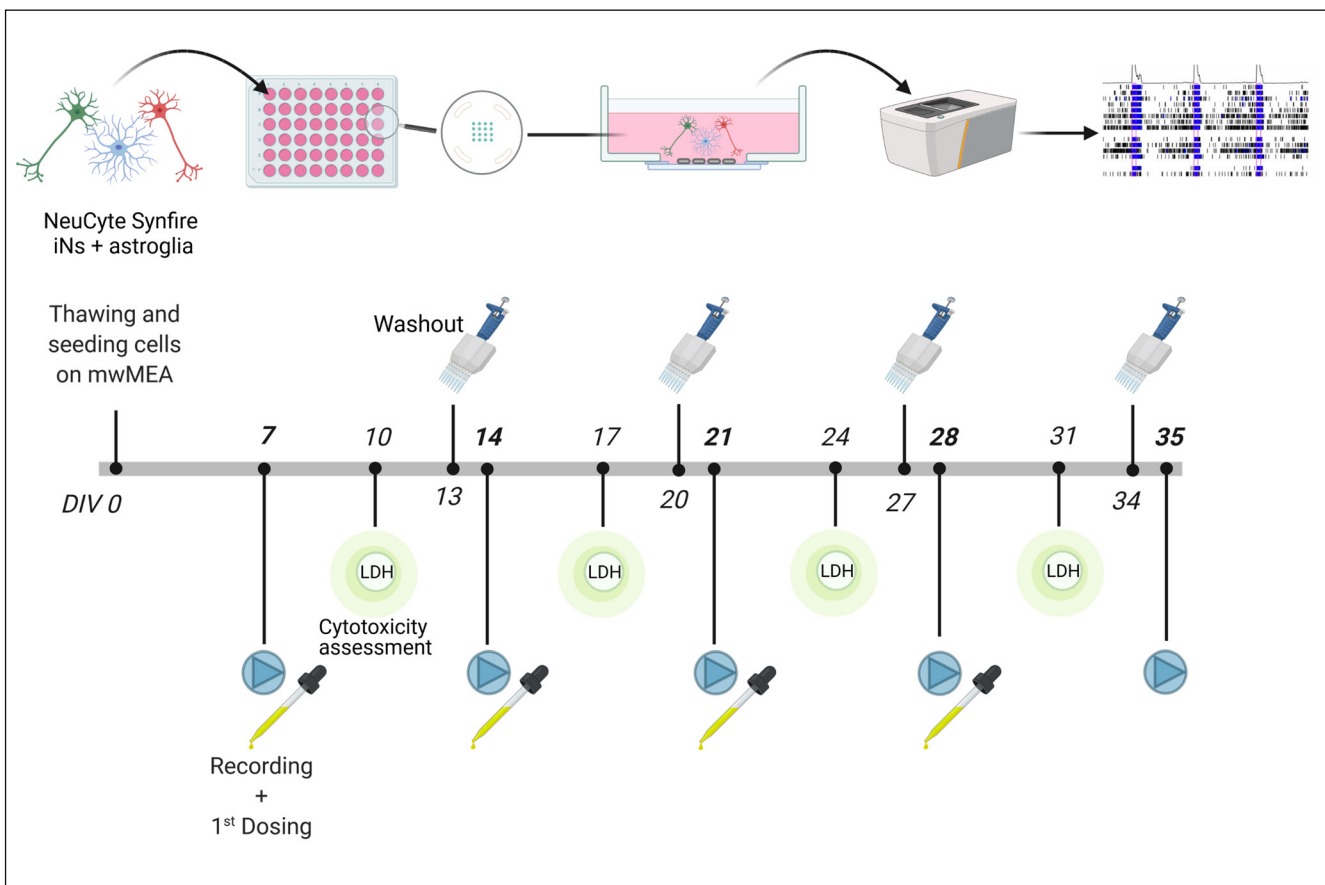


**Fig. 1: Experimental setup of the human NNF assay**

A co-culture of hiPSC-derived excitatory and inhibitory neurons and primary astroglia (NeuCyte, USA) was plated in a defined cell type ratio on 48-well MEA plates at DIV 0. Cultures were allowed to mature for 7 days before exposure to the test compounds. 24 h before the weekly recording of spontaneous electrical network activity on DIV 7, 14, 21, 28, and 35 a washout of the respective compounds was performed. Additionally, cytotoxicity was assessed every week on DIV 10, 17, 24, and 31 three days after dosing. Created with BioRender.com.

#### Cell culture

SynFire glutamatergic neurons (Lot#000172 and 000131), SynFire GABAergic neurons (Lot#000172 and 000131), and SynFire astrocytes (Lot#13029-050 and 00190820; all from NeuCyte, USA) were thawed and cultured according to the manufacturer's protocol. In short, all three cell types were thawed and resuspended in a defined ratio in supplemented seeding medium (NeuCyte), resulting in a co-culture consisting of induced neuronal (iN) and glial cells (iN:glia). Cells were seeded at a density of  $270 \times 10^3$  cells/well ( $140 \times 10^3$  glutamatergic neurons,  $60 \times 10^3$  GABAergic neurons,  $70 \times 10^3$  astrocytes) on 48 well MEA plates (Axion M768-KAP-48) pre-coated with 0.1% polyethyleneimine and 20 µg/mL mouse laminin. This approach resulted in a cell type ratio of 52% glutamatergic neurons, 22% GABAergic neurons, and 26% astroglia. The seeding was performed in a 50 µL droplet ( $270 \times 10^3$  cells/droplet) of supplemented seeding medium (NeuCyte) per well. After cells were allowed to adhere for 24 h, each well was filled with 250 µL supplemented short-term medium (NeuCyte). At days *in vitro* (DIV) 3 and 5, cells were fed by replacing half of the medium with supplemented short-term

medium. From DIV 7 onwards, medium was gradually changed to supplemented long-term medium (NeuCyte) by replacing half of the medium on DIV 7 and 10 until the medium was completely replaced at DIV 13 (washout). The short-term medium is supplemented with a substance that reduces the proliferation of astroglia.

Following the same plating procedure and seeding density, 20 wells of a pre-coated 96-well flat bottom plate (Greiner) were prepared for weekly cytotoxicity assessments.

#### Experimental design

Following the first recording of spontaneous electrical network activity at DIV 7, cells were exposed to the respective test compound by exchanging half of the medium with supplemented long-term medium containing double-concentrated compound. Half medium changes with the compounds were conducted at DIV 10, 17, 24, and 31. The removed medium was used for cytotoxicity assessment described below. 24 h before weekly recordings at DIV 7, 14, 21, 28, and 35, a washout with PBS was performed prior to replacing the medium with chemical-free



supplemented long-term medium to minimize acute substance effects during MEA recordings. For this purpose, the medium was completely removed and replaced by adding 300 µL pre-warmed PBS. After incubation for 30 min (37°C, 5% CO<sub>2</sub>), PBS was replaced by freshly supplemented long-term medium. After recording, the medium was again replaced with long-term medium containing the test compound. Two compounds were tested per 48-well MEA plate including solvent and endpoint-specific controls. Each independent experiment (biological replicate) results from a different thawing procedure done on a different day and comprises three technical replicates (replicate wells, see Fig. S1<sup>1</sup>). In this study, we followed a two-step testing paradigm, where each compound was initially tested twice independently. If the two independent experiments showed the same results, e.g., no effect, no additional experiment was conducted. In case of conflicting outcomes, a third experiment was performed. The experimental setup is summarized in Figure 1.

#### *MEA recording*

Spontaneous electrical network activity on DIV 7, 14, 21, 28, and 35 was recorded with the Axion Maestro Pro system, a 768-channel amplifier, and AxIS software version 1.5.3 or later (Axion Biosystems, Atlanta, USA). The recording procedure of the electrical network activity was composed of a 15-min equilibration period and two consecutive measurements of 15 min each, whereas only the last 15-min recording was used for further analysis. The last pipetting (washout) was performed 24 h prior to the measurement. For acute response measurements (CNQX, BIC), pipetting was performed right before the measurement, with a 5-min wash-in phase, and only the first 15 min recording was analyzed. All recordings were conducted at 37°C and 5% CO<sub>2</sub>. The activity was measured using a gain of 1000x and a sampling frequency of 12.5 kHz. A Butterworth band-pass filter was used (200-3000 Hz) prior to spike detection (threshold of 6x root mean square [RMS] noise on each electrode) via the AxIS adaptive spike detector. An active electrode was defined as ≥ 5 spikes/min.

#### *Cytotoxicity assessment*

Cytotoxicity was assessed every week and three days after re-dosing (at DIV 10, 17, 24, and 31) using the CytoTox-ONE Homogeneous Membrane Integrity Assay, which is based on measurement of lactate dehydrogenase (LDH) release, according to the manufacturer's instructions (#G7891, Promega, Madison, United States). 50 µL medium from each well was removed, transferred to a 96-well plate (Sarstedt), and 50 µL CytoTox-ONE reagent was added. 30 min prior to the cytotoxicity assay, three wells of the lysis plate were treated with 10% Triton-X 100, and the supernatant was used as lysis positive control. As a background control, 50 µL of supplemented long-term medium was incubated with the same volume of CytoTox-ONE reagent. Following 2 h of incubation at room temperature, the fluorescence was detected with a Tecan infinite M200 Pro reader (ex: 540 nm; em: 590 nm).

#### *Data analyses*

After recording with the AxIS software, recordings were re-recorded using the same software, resulting in .spk files. For single electrode burst detection, the inter-spike interval threshold algorithm was used with a maximum inter-spike interval of 100 ms with at least five spikes. Additionally, network bursts were detected using the Axion Neural Metric Tool and the envelope algorithm with a threshold factor of 1.5, a minimum inter-burst interval of 100 ms, and 60% active electrodes. The synchrony window was set to 20 ms. This resulted in 72 network parameters for five time points and seven concentrations. As a manual evaluation of all 72 parameters was not possible, an automated evaluation workflow that calculates the trapezoidal area under the curve (AUC) and benchmark concentrations (BMC) was set up. AUC was calculated as previously described by Brown and colleagues (Brown et al., 2016). Consecutively, spline interpolations with degree 1 polynomials for the data points given for conditions were made for each endpoint in each plate. If the response for an endpoint for the DIV 7 measurement was missing, e.g., because of absent bursting activity in an active well, it was set using random sampling throughout overall available first DIV responses for that endpoint on the same plate when at least 50% of these responses were available. In the final pre-processing step, a common time duration, related to one DIV, with available responses in the resulting data was determined for each endpoint and experiment. Finally, the AUC from these common durations was determined.

The pesticide data presented in this paper were derived from two to three individual experiments per compound as stated in Table S1<sup>1</sup>. The data was normalized to the median solvent control and re-normalized to the starting point of a concentration-response curve generated with the R package drc<sup>2</sup> as described below. For cytotoxicity data, a different normalization was used: The normalized cytotoxicity response equaled the lysis control (LC) median minus the response of the respective concentration divided by the lysis control median minus the solvent control (SC) median:

$$\text{normalized response} = \frac{\text{LC}(\text{median}) - \text{response}}{\text{LC}(\text{median}) - \text{SC}(\text{median})} \quad (\text{Eq. 1})$$

BMCs (BMC<sub>50</sub> and BMC<sub>50ind</sub>) with their upper and lower confidence intervals (CI) were calculated based on the R package drc<sup>2</sup>. Linear, sigmoidal, monotonic, and non-monotonic models were run with the concentration-response data of each endpoint, and Akaike's information criteria were used to determine the best fit. Endpoints were classified as DNT-specific if CIs of the BMCs calculated for the DNT-specific endpoint did not overlap with the cytotoxicity endpoint. If the overlap exceeded 10%, the endpoint was classified as unspecific. Statistical significance was calculated using GraphPad Prism 8.2.1 and one-way ANOVA with Dunnett's post-hoc tests or two-tailed Student's t-tests ( $p \leq 0.05$  was termed significant).

<sup>2</sup> <https://cran.r-project.org/web/packages/drc/index.html>



### RNA-Seq

NeuCyte's iPSC-derived glutamatergic and GABAergic-induced neurons and human astrocytes were seeded to form iN:glia co-culture. Cells were harvested on DIV 7, 14, 21, 28, and 35, four biological replicates per time point. RNA-Seq was performed by Novogene (CA, USA). Total RNA was extracted using the Qiagen RNA Extraction Kit (Qiagen, Germany). For library preparation, NEBNex<sup>®</sup> Ultra<sup>TM</sup> II RNA Library Prep Kit for Illumina<sup>®</sup> was used (New England Biolabs, MA, USA). For sequencing, NovaSeq 6000 was used, utilizing paired-end 150 bp read length. Downstream data analysis was performed using a combination of programs. Alignments were parsed using STAR program. Reads were aligned to the reference genome GRCh37 using STAR (v2.S). STAR counted number of reads per gene while mapping. The counts coincide with those produced by HTseq-count with default parameters. Then fragments per kilobase per million mapped reads (FPKM) of each gene were calculated based on the length of the gene and read counts mapped to this gene.

### Immunostainings

SynFire iN:glia co-cultures were validated by immunostaining of markers including: guinea pig anti-MAP2 (1:200, Synaptic Systems, 188 004), rabbit anti-synapsin1 (1:200, Synaptic Systems, 106 008), rabbit anti-VGLUT2 (1:200, Synaptic Systems, 135 403), rabbit anti-VGAT (1:200, Synaptic Systems, 131 011), rabbit anti-GFAP (1:250, Abcam, ab4674). Secondary antibodies were conjugated to AlexaFluor647 (1:200, Invitrogen) and AlexaFluor488 (1:200, Invitrogen).

On DIV 35, the co-cultures were fixed with 4% paraformaldehyde (Sigma Aldrich) at room temperature for 15 min, washed three times with PBS (PAN Biotech), and then incubated overnight at 4°C with primary antibodies diluted in blocking solution (5% goat serum (Sigma Aldrich) + 0.2% Triton X-100 (Sigma Aldrich) in PBS). On the second day, co-cultures were washed three times with PBS and then incubated with secondary antibodies diluted in blocking solution with 1% Hoechst 33258 (1:100, Merck). After washing three times with PBS, fluorescence imaging was performed using an automated microscope system for high-content imaging (CellInsight CX7 LZR Platform, Thermo Fisher Scientific, Waltham, MA, USA).

## 3 Results

**Characterization of an MEA-based assay for network formation**  
The present study describes the establishment and characterization of a human iPSC-based NNF assay. The assay was challenged with 27 pesticides and acetaminophen as a negative control. Cells of a defined cell type ratio (52% glutamatergic neurons, 22% GABAergic neurons, 26% astrocytes) were seeded as a monolayer culture on each MEA well containing 16 electrodes.

Figure 2 illustrates immunocytochemical staining of the neural networks on DIV 35 as well as their characteristics at different

maturity time points (DIV 7-35) using transcriptome profiling (RNA-Seq). DIV 35 staining (Fig. 2A) showed a strong presence of MAP2-positive neurons and a lower amount of NeuN (*RBFOX3*), indicating a high maturation level of the networks. The glial marker GFAP was strongly expressed, and the co-cultures were positive for the pre-synaptic marker synapsin, the vesicular GABA transporter vGAT, and the vesicular glutamate transporter vGLUT.

These characteristics were confirmed by RNA sequencing of co-cultures at different time points (Fig. 2B). The maturation of neurons within the system was verified by a high expression of neuronal maturation markers, e.g., *MAP2* (Maccioni and Cambiazo, 1995), *DLG4*, and *SYP* (Glantz et al., 2007), compared to genes coding for immature neurons, e.g., *NEUROD1* (Seki, 2002). Additionally, the high expression of *GFAP* and *AQP4*, compared to *S100B*, characterizes the mature glial system (Holst et al., 2019). Also, genes coding for GABA and AMPA receptors and glutamate transporters showed expression at DIV 7 with gradations within their subtypes (e.g., *SLC1A2* vs. *SLC1A3*). Voltage- (VG) and ligand-gated (LG) ion channels were enriched in the culture. In comparison to VG- and LG-calcium channels, VG-sodium channels were more highly expressed. Moreover, expression of transcripts coding for dopaminergic, cholinergic (nicotinic and muscarinic), and NMDA receptors (NMDAR) were detected. Especially *CHRNA3* (Karlin, 2002) and *DRD2* (Missale et al., 1998) expression was enhanced at DIV 7 and decreased with increasing maturation of the networks. The higher expression of *SLC12A5* (*KCC2*) compared to *SLC12A2* (*NKCC1*) at DIV 14 indicates that the cells had passed the GABA switch, which marks the shift from pre-mature excitatory to mature inhibitory GABAergic neurons (Leonzino et al., 2016). Taken together, the gene expression data show that the neural networks develop over time and express a broad variety of genes related to neuronal and glial function, which is a prerequisite for neural network function.

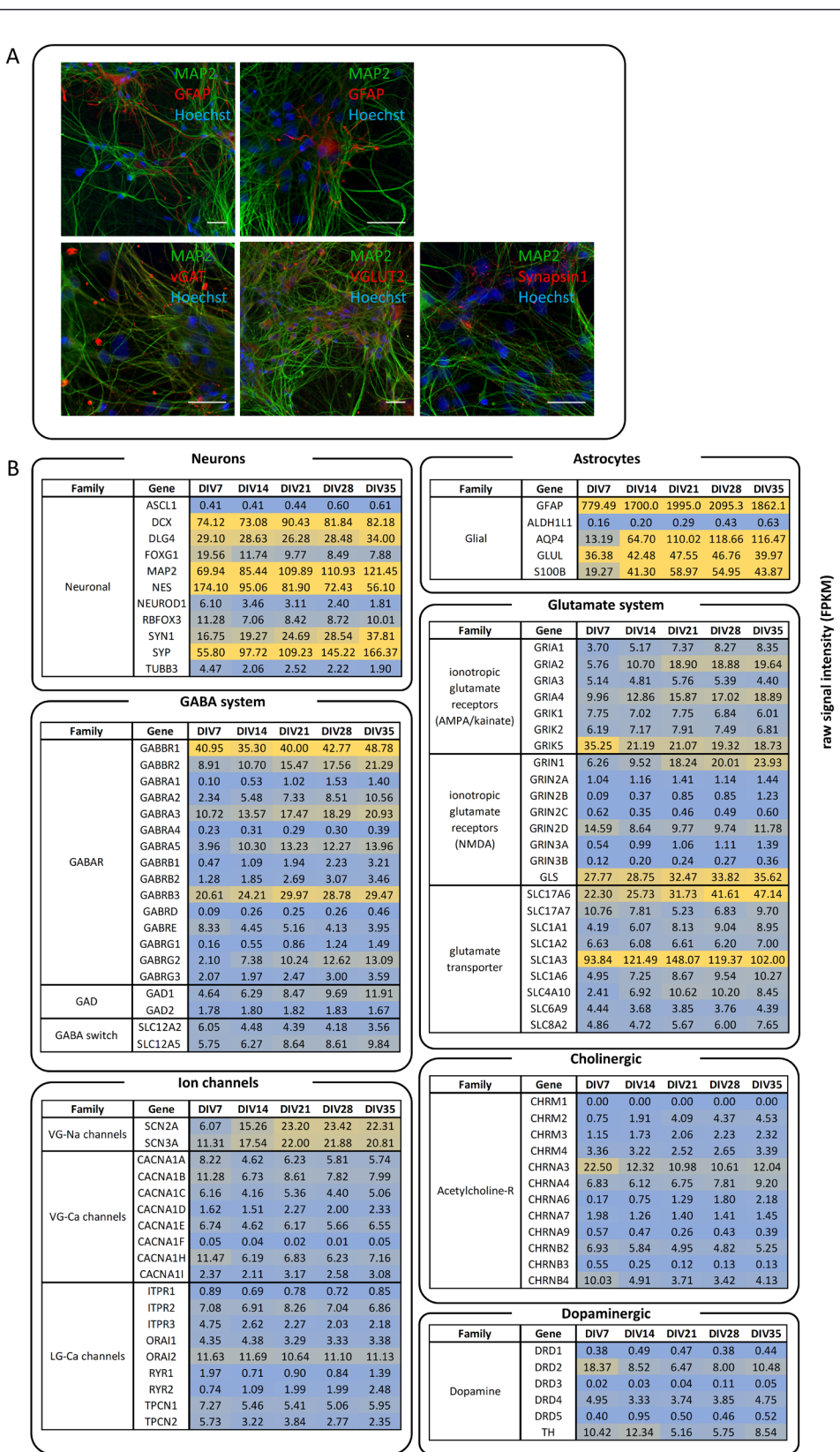
MEA are important tools to study network electrophysiology. MEA recordings provide high-content data based on the recording of extracellular action potentials, so-called spikes, which are the basic unit of activity of a neural network. During the development of a network, spikes can group into bursts and can synchronize their activity, resulting in network bursts. To confirm the contribution of functional GABAergic and glutamatergic neurons in the development of the networks, we performed an acute pharmacological modulation of neural networks on DIV 21 by challenging the neuronal subtypes with the receptor antagonists BIC and CNQX. BIC is a well-studied GABA<sub>A</sub> receptor antagonist, which primarily competitively inhibits binding of GABA to its receptors. As a consequence, BIC reduces GABA-activated conductance by reducing channel opening times as well as opening frequency, resulting in an increased firing rate (Macdonald et al., 1989; Johnston, 2013; Mack et al., 2014). In comparison, CNQX primarily antagonizes AMPA-type glutamate receptors and thereby suppresses spontaneous excitatory glutamatergic synap-



**Fig. 2:**  
Immunocytochemical staining and gene expression profiles of SynFire neuronal/glial co-cultures at different maturation time points

(A) Immunocytochemical staining of different neuronal and glial markers of differentiated co-cultures on DIV 35. Nuclei were stained with Hoechst (blue) together with MAP2 (green) and either GFAP, synapsin1, vGAT or vGlut, respectively (red). Scale bar = 50 µm.  
(B) RNA-Seq data was used to generate gene expression profiles on DIV 7, 14, 21, 28, and 35. Values are presented as fragments per kilobase per million mapped reads (FPKM). Cut-off for likely expression: 2.78 FPKM.

VG, voltage-gated;  
LG, ligand-gated;  
Ca, calcium; Na, sodium



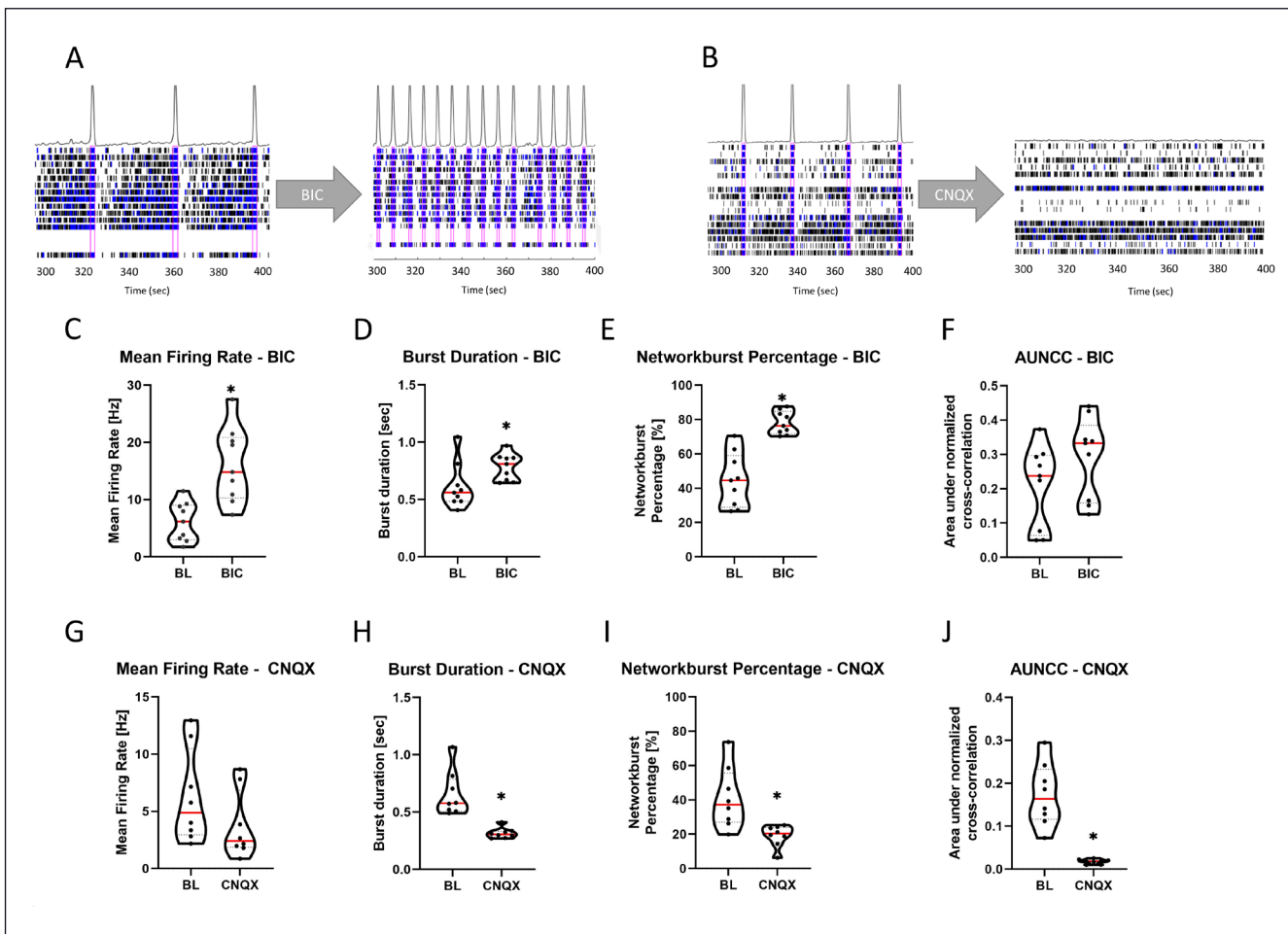


**Fig. 3: Acute pharmacological modulation of DIV 21 neural network activity**

Untreated DIV 21 neural networks (baseline, BL) were exposed to 3  $\mu$ M bicuculline (BIC) or 30  $\mu$ M cyanquinaline (6-cyano-7-nitro-quinoxaline-2,3-dione; CNQX), respectively. (A, B) 100-s spike raster plots reveal the effects of 3  $\mu$ M BIC or 30  $\mu$ M CNQX on DIV 21 neural networks. Spikes are represented as black bars, bursts as blue bars. Pink boxes indicate network bursts. (C-F) 3  $\mu$ M BIC enhanced neural network activity as indicated by the increase in different network parameters compared to the baseline. (G-J) 30  $\mu$ M CNQX decreased neural network activity as measured by the decrease in different network parameters. Data are represented as violin plot distributions of 9 (C-F) or 8 (G-J) independent experiments. Dotted lines represent quartiles of distribution, and red bars represent the median. Statistical significance was calculated using two-tailed Student's t-tests. A p-value below 0.05 was termed significant. \*, significant compared to the respective BL.

tic activity (Neuman et al., 1988; Odawara et al., 2016). After baseline recording at DIV 21, cells were exposed to the respective modulator, and the electrical activity was measured. Exposure to 3  $\mu$ M BIC increased general electrical activity, especially synchronous bursting (Fig. 3A, pink boxes), whereas 30  $\mu$ M CNQX led to a loss of organized activity, as illustrated by representative 100-s spike raster plots (Fig. 3A,B). For additional quality control of the test method, acute treatments with the two described modulators were included in every assay run. Violin plots for each compound and four different network parameters (Fig. 3C-F) illustrate the distribution of these data, and the median of 8-9 independent experiments (median of 3 technical replicates each) reveals the effect of both receptor antagonists.

3  $\mu$ M BIC significantly enhanced the mean firing rate and burst duration. Consistent with the spike raster plots, BIC doubled the percentage of overall spikes contributing to network bursts from 40% to 80% ("Network burst percentage", Fig. 3E) and increased the area under normalized cross-correlation ("AUNCC", Fig. 3F), which describes the synchronicity of the network. In contrast, CNQX inhibited the overall activity and organization of the networks. Especially burst duration and synchronicity were impaired with a low degree of variation (Fig. 3H,J).

As already indicated by gene expression data (Fig. 2), electrophysiological measurements over time confirmed maturation of the neural networks based on their display of specific firing patterns like organized spiking and synchronicity at later stages of differen-

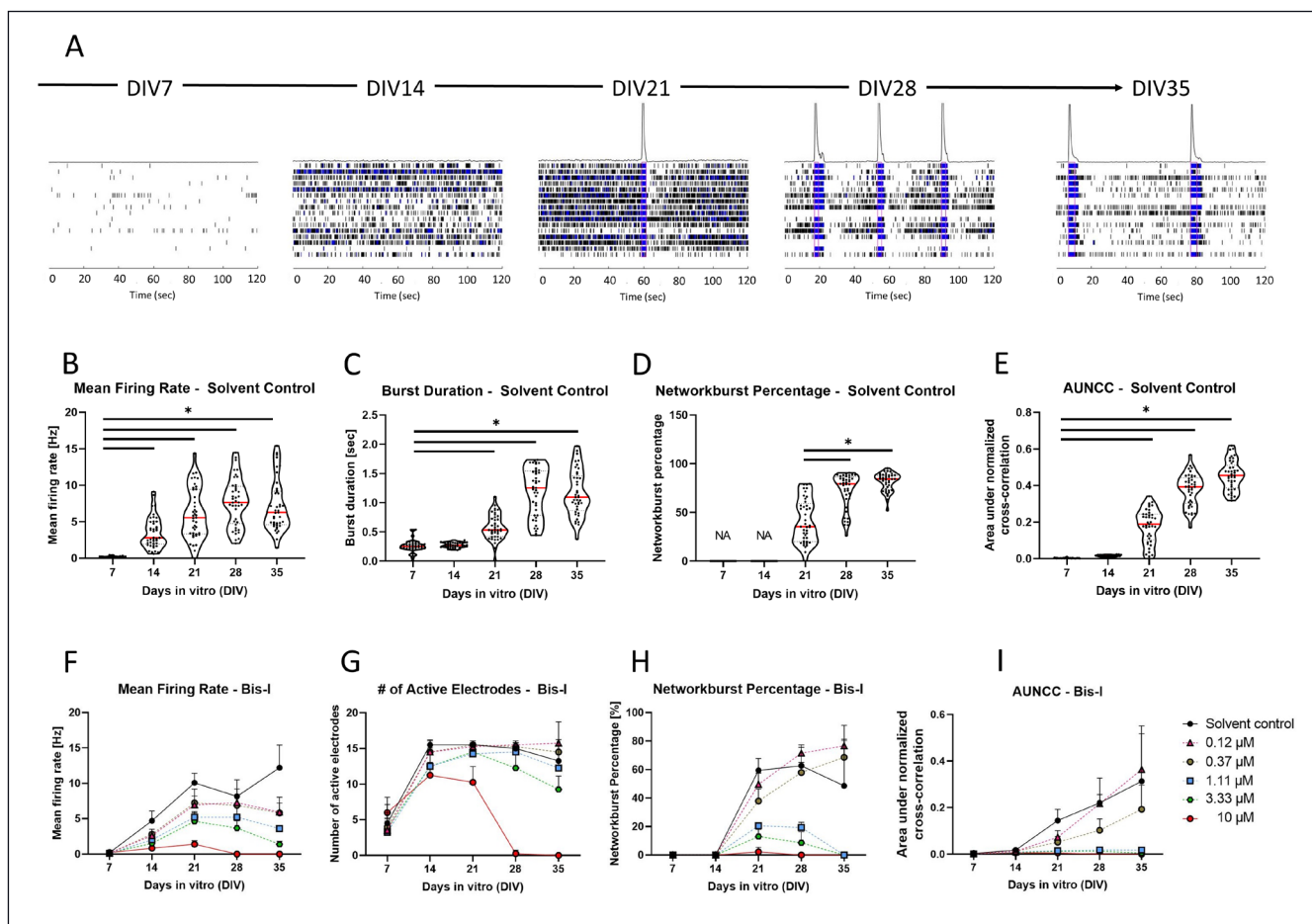


**Fig. 4: Neural network development on 48-well microelectrode arrays (MEA) and its inhibition by bisindolylmaleimide I (Bis-I)**  
(A) Representative 120 s spike raster plots referring to DIV 7 to 35. Spikes are represented as black bars, bursts as blue bars. Pink boxes indicate network bursts. (B-E) Dot plots showing the distribution of untreated (solvent control; 0.1% DMSO) network activities from DIV 7 to 35 over four network parameters (mean firing rate, burst duration, network burst percentage, and area under normalized cross-correlation (AUNCC)). Single dots represent the median of three replicates of each experiment. The red bar defines the median over all plates ( $n = 41$ ). (F-I) Starting at DIV 7, networks were treated with increasing concentrations (0.12; 0.37; 1.11; 3.33 and 10  $\mu$ M) of the PKC inhibitor Bis-I. Different network parameters (mean firing rate, number of active electrodes, network burst percentage, area under normalized cross-correlation (AUNCC)) reflect the impairment of Bis-I on neural network development over 35 days of differentiation. Data are shown as mean  $\pm$  SD of four wells. Statistical significance was calculated using one-way ANOVA. A p-value below 0.05 was termed significant. \*, significant compared to the earliest DIV.

tiation (Fig. 3A). Representative spike raster plots illustrate these features over the 35-day development of the networks (Fig. 4A). At DIV 7, spikes (black bars) were the sole form of activity, whereas at DIV 14, bursts (blue bars) started to form on single electrodes. Along with the increase in bursting activity and the emergence of a synchronous network starting on DIV 21, the number of spikes between network bursts decreased at DIV 28 and 35. This transition in network development is reflected by the evaluation of different network parameters of untreated solvent control wells (0.1% DMSO) from all plates contributing to this study ( $n = 41$  plates and 123 wells). Figure 4B-E shows the distribution of different parameters between experiments (each data point reflects the median of 3 wells of each independent experiment) and indicates the variation

of the hNNF assay. On DIV 7 and 14, the mean firing rate was notably below 5 Hz, but then rose to 10 Hz, with its peak at DIV 28 (Fig. 4B). The same trend was observed for the duration of bursts between DIV 7 and 35 (Fig. 4C). Nevertheless, some parameters, like the network burst percentage or the AUNCC, continuously increased until DIV 35 (Fig. 4D,E). Because the highly organized activity of the network is rarely observed at DIV 7 and 14 (Fig. 4E), network burst parameters were only considered from DIV 21 to 35 for the following evaluations.

To show that neural network development within the hNNF assay can be altered by a specific mechanism, DIV 7 networks were exposed to different concentrations of the PKC inhibitor Bis-I following the exposure scheme described in Figure 1. Bis-I inhibited

**Tab. 1: 14 Parameters from MEA recordings and their respective inter-experimental variability as coefficient of variation (COV)**

Category	Parameter	Definition	Inter-experimental COV
General activity	Mean firing rate	Total number of spikes divided by the duration of the analysis (Hz)	28.45
	Number of active electrodes	Number of electrodes with activity > 5 spikes/min	9.97
	Number of bursting electrodes	Total number of electrodes within the well with bursts/min greater than the burst electrode criterion (min # of spikes: 5; max ISI: 100 ms)	11.14
Bursting activity	Burst duration	Average time from the first spike to last spike in a single-electrode burst	11.24
	Number of spikes per burst	Average number of spikes in a single-electrode burst	25.17
	Mean ISI within burst	Mean inter-spike interval, time between spikes, for spikes in a single-electrode burst	5.94
	Inter-burst interval	Average time between the start of single-electrode bursts	19.18
	Burst frequency	Total number of single-electrode bursts divided by the duration of the analysis (Hz)	28.60
Connectivity	Burst percentage	Number of spikes in single-electrode bursts divided by total number of spikes, multiplied by 100	14.67
	Network burst frequency	Total number of network bursts divided by the duration of the analysis (Hz)	20.83
	Network burst duration	Average time from the first spike to last spike in a network burst	11.42
	Network burst percentage	The number of spikes in network bursts divided by the total number of spikes, multiplied by 100	7.08
	Number of spikes per network burst	Average number of spikes in a network burst	29.01
	Area under normalized cross-correlation (AUNCC)	Area under the well-wide pooled inter-electrode cross-correlation normalized to the auto-correlations	14.73

neurite outgrowth in PC-12 cells (Das et al., 2004), rat cortical neurons, and hiPSC-derived neurons (Druwe et al., 2016). Furthermore, *in vitro* MEA experiments showed decreased firing and bursting rates of rat neural networks after Bis-I exposure (Robinette et al., 2011). We observed that network activity was affected by Bis-I in a concentration-dependent manner, as illustrated by representative network parameters in Figure 4F-I. Untreated controls showed a mean firing rate of more than 10 Hz on DIV 35, whereas Bis-I interfered with the formation of a functional network starting at low concentrations of 0.12 µM, resulting in about 5 Hz (Fig. 4F). Exposure to 10 µM Bis-I resulted in a fully muted network at DIV 28 and DIV 35 regarding all four displayed network parameters. The network burst percentage was also reduced to 20% at DIV 21 and 28 by 1.11 µM Bis-I and to 0% at DIV 35 (Fig. 4H). This impairment in network bursting is also reflected in the AUNCC (Fig. 4I). After this initial proof-of-concept, Bis-I was introduced as an endpoint-specific positive control for the hNNF test method. For this purpose, each experimental run in the compound screening contained control wells treated with 5 µM Bis-I. The data of 13 independent experiments (39 wells) showed that Bis-I reliably and significantly inhibits different network parameters, e.g., burst duration, network burst percentage, and network synchronicity (AUNCC, Fig. S2<sup>1</sup>). The overall effect

of Bis-I on the mean firing rate was not statistically significant, which may be due to the higher variability of this parameter, as explained in the next section (see Fig. S2<sup>1</sup>).

#### *Selection of parameters to evaluate*

MEA recordings generated in this study result in 72 network parameters, which are predominantly correlated and can be grouped into spike-, burst- and network-related parameters. A plethora of these define the same characteristic of the network (e.g., “mean firing rate” and “weighted mean firing rate”) or use a different statistical method to describe the parameter (e.g., “inter-burst interval-Avg” vs “inter-burst interval (median)-Avg”). The evaluation of one 48-well MEA plate during a time course of 35 days results in over 17,000 data points, which makes the processing of data and interpretation of possible compound effects enormously challenging. To reduce the number of data points and only concentrate on the most informative and at the same time robust parameters, we analyzed the variability of all parameters across all wells treated with the lowest concentration of each test compound. To this end, we calculated the inter-experimental variability for each parameter by merging the endpoint responses of the lowest concentrations of independent experiments relative to the solvent control and normalizing these. Afterwards, we derived

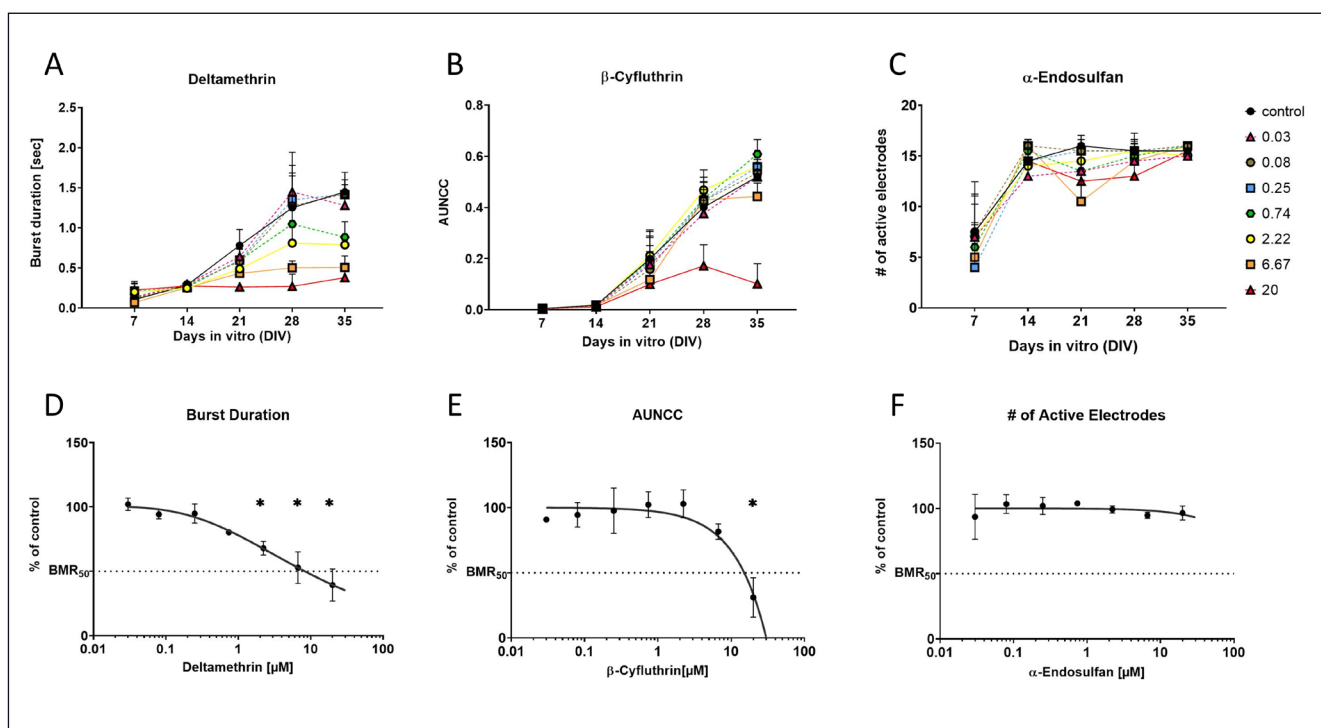


**Fig. 5: Example data for area under the curve (AUC) summary of time- and concentration-dependent MEA readouts**

(A-C) Starting at DIV 7, neural networks were treated with increasing concentrations of deltamethrin (A),  $\beta$ -cyfluthrin (B), and  $\alpha$ -endosulfan (C), and exemplary network parameters were evaluated. Time- and concentration-dependent data are shown as the mean of three (A, B) or two (C) independent experiments  $\pm$  SEM (A, B) or SD (C). AUC values were computed for these data and plotted in a concentration-dependent relationship (D-F). Compounds did not induce cytotoxicity (data not shown). Data are represented as the mean of three (D, E) or two (F) independent experiments  $\pm$  SEM (D, E) or  $\pm$  SD (F). Replicates within one experiment are summarized by median. Curve fitting was conducted as described in Section 2. Statistical significance was calculated using one-way ANOVA. A p-value below 0.05 was termed significant. \*, significant compared to the respective solvent control.

the inter-experimental variability as the coefficient of variation (COV) of these collections of data points for each compound. The higher the COV, the greater is the dispersion. Additionally, we included parameters that were previously described in the literature (Brown et al., 2016; Frank et al., 2017; Kosnik et al., 2020) and represent a broad variety of network development characteristics. We then selected a final set of 14 network parameters that cover the three categories “general activity”, “bursting activity”, and “connectivity” of neural networks and have a COV between 6 and 29 (Tab. 1).

#### Concentration-dependent effects of pesticides on network activity

After having set up the hNNF assay by defining a treatment scheme and standard operating procedure, establishing an endpoint-specific control, and evaluating variability over wells and plates, we next applied the hNNF assay to screen 28 chemicals. The set consists of 27 pesticides plus acetaminophen as a negative control compound. To identify concentration-dependent effects of substances that impaired neural network formation, cells were exposed weekly from DIV 7 to 35, including respective washout steps 24 h before each recording. As an example, deltamethrin and

$\beta$ -cyfluthrin reduced the mean firing rate (Fig. 5A) and AUNCC (Fig. 5B) of neural networks, respectively, in a time- and concentration-dependent manner without inducing cytotoxicity. Acibenzolar-S-methyl, on the other hand, did not affect the number of active electrodes (Fig. 5C). These time-concentration relationships can be translated into concentration-response curves as illustrated in Figure 5D-F. For each concentration, the trapezoidal AUC was calculated to include all five time points in one single value per concentration. This approach, adapted from Brown et al. (2016) and Shafer (2019), simplifies the comparison of effects over different days of neural network development. In the next step, the AUC information and resulting concentration-response curves were used to estimate BMCs with upper and lower confidence limits for each compound and parameter. For estimation of the BMCs, a benchmark response (BMR) of 50% ( $BMR_{50}$ ) was selected as this best reflects the variability of the most variable parameters (see Tab. 1).

Figure 6 summarizes the concentration-dependent effects of the 28 tested compounds on neural network development that produced a 50% change (reduction or induction) from the curve’s starting point. Five of the 14 network parameters were not affected by any compound, including number of active electrodes and

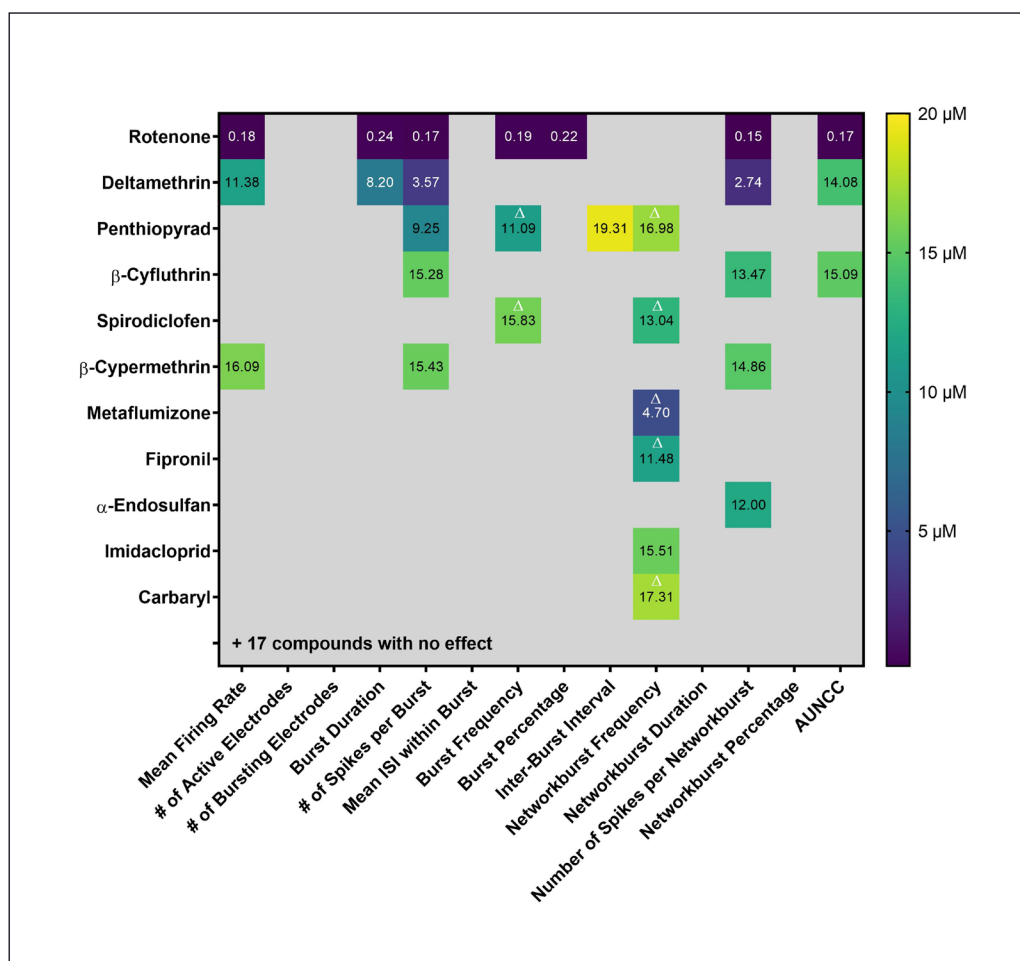


**Fig. 6: Summary of BMCs across 14 network parameters of the hNNF assay**

No cytotoxicity was observed. 17 compounds had no effect (acetaminophen, acetamiprid, acibenzolar-s-methyl, aldicarb, chlorpyrifos, chlorpyrifos-methyl, clothianidin, diazinon, dimethoate, dinotefuran, disulfoton, etofenprox, flufenacet, methamidophos, thiacloprid, thiamethoxam, triallate; data not shown).

$\Delta$ , induced effects; numbers are given in  $\mu\text{M}$ . No value assumes BMCs > 20  $\mu\text{M}$  ( $> 0.3 \mu\text{M}$  for rotenone). Confidence intervals are listed in Table S2<sup>3</sup>. AUNCC, area under normalized cross-correlation.

mean inter-spike interval within bursts. 17 compounds tested negative, e.g., acetaminophen, chlorpyrifos, and its derivate chlorpyrifos-methyl (data not shown). 11 of the 27 pesticides are considered positive, for which at least one network parameter had to be affected without cytotoxic effects at any administered concentration.  $\beta$ -Cyfluthrin,  $\beta$ -cypermethrin, deltamethrin, penthiopyrad, and rotenone evoked effects in more than two parameters, whereas the other six pesticides affected one or two parameters. Network burst frequency was the most sensitive parameter with six hits, of which five represent inductive effects. Furthermore, spirodiclofen and penthiopyrad additively increased the burst frequency. Predominantly, the observed effects are all in a similar range between 9 and 20  $\mu\text{M}$ . In contrast, deltamethrin and metaflumizone influenced different network parameters below 9  $\mu\text{M}$ . Rotenone is denoted as the most potent compound, specifically reducing seven parameters in a concentration range between 0.15 and 0.24  $\mu\text{M}$  without causing cytotoxicity. The network parameter connectedness, e.g., burst rate and mean firing rate, seen after rotenone treatment is not visible for all compounds. This might be due to parameters compensat-

ing each other, like penthiopyrad decreasing the number of spikes per burst and increasing the burst frequency at the same time or BMCs being close to the upper testing limit, like for  $\beta$ -cyfluthrin.

#### 4 Discussion

In the last years, scientists from academia, industry, and regulatory authorities across the world agreed on the need for a standardized *in vitro* testing strategy, aiming for a cheaper and faster generation of additional data for DNT hazard assessment (EFSA, 2013; Crofton et al., 2014; Bal-Price et al., 2015, 2018; Fritzsche et al., 2017, 2018a,b). This resulted in the compilation of a DNT IVB, which includes various test methods covering different KEs of neurodevelopment, including the formation and function of neural networks (Fritzsche, 2017; Fritzsche et al., 2017; Bal-Price et al., 2018). One of the gaps identified in the DNT IVB is the assessment of network formation and function in a human-based cell model (Crofton and Mundy, 2021). To fill this gap, we estab-

<sup>3</sup> doi:10.14573/altex.2206031s2



lished the human neural network formation assay (hNNF), which consists of hiPSC-derived excitatory and inhibitory neurons and primary astroglia (SynFire, NeuCyte, USA). The functionality of neuronal subtypes and the ability of the cell model to detect alterations via a known MoA were confirmed by pharmacological modulation. When challenged with a test set of 28 substances, the assay revealed compound-specific effects of different pesticides on network development.

#### 4.1 Assay establishment

Under most circumstances, newly developed methods for DNT testing are restricted by their inability to test large numbers of chemicals (Coecke et al., 2007; Crofton et al., 2011). To tackle this issue, Crofton et al. (2011) provided a set of 15 principles aiming to enhance assay amenability to higher throughput screening. The establishment of the hNNF assay in this study was realized by considering these principles, which are described in more detail in the following (P1-15). During early brain development, neurons start to mature and build connections via synapses (Okado et al., 1979; Zhang and Poo, 2001). Neural network formation and function is therefore a key aspect of neurodevelopment (P1 “Key event of neurodevelopment”). By measuring extracellular local field potentials on MEAs, network formation and function can be assessed, thus providing information on electrical activity, firing patterns, and synchronicity of the neural networks (P2 “Endpoint measurement”). By calculating the AUC for each concentration and normalizing the values to the respective solvent control, the hNNF assay can reflect alterations of network activity in both directions (increase and decrease; P3 “Dynamic range”). Furthermore, Crofton et al. (2011) emphasize the importance of parametric controls, meaning parameters of the assay that evoke predictable changes in the endpoint (P4 “Parametric controls”). One aspect that was confirmed within the presented study is the increase in electrical activity and synchronicity of the networks with increasing culture time (Fig. 3). Furthermore, Saavedra and colleagues showed that an excitatory:inhibitory (ex:inh) ratio of 70:30 using SynFire neurons exhibits the steadiest spiking increase and coverage of electrodes over differentiation time compared to other ex:inh ratios (Saavedra et al., 2021). Principle 5 (“Response characterization”) highlights the relevance of a precise effect characterization, based on the degree of variability in the assay. As recommended by the EFSA Scientific Committee, the BMC approach was applied to derive a reference point or point of departure (Hardy et al., 2017), whereby the BMR should be defined as an effect size that is higher than the general variability of the measured endpoint. Based on the inter-experimental standard deviation (1.5\*COV), which was calculated for every parameter presented in this study (Tab. 1), we defined the BMR<sub>50</sub> (reduction) and BMR<sub>50ind</sub> (induction) as the degree of change that, if exceeded, results in a positive response (hit). Furthermore, Crofton and colleagues (2011) state that the concentration range covered, and the resulting concentration-response, play a highly significant role in terms of comparison of sensitivity between different endpoints. For this study, we selected a concentration range that has already been used in other *in vitro* DNT assays and has elicited

little to no cytotoxicity (Frank et al., 2017; Masjosthusmann et al., 2020; Blum et al., 2022). To discriminate specific from unspecific effects, we assessed the cytotoxicity of each compound on a weekly level during the 35-day culture period (P7 “Endpoint selectivity”). Another crucial requirement for assay development is the selection of endpoint-specific controls, altering the endpoint by known MoA both negatively and positively. In the present study, Bis-I, a PKC inhibitor was selected as an endpoint-specific control (P8 “Endpoint-selective controls”). In primary rat cortical cells, the inhibition of PKC blocked the local astrocytic contact and thus the facilitation of excitatory synaptogenesis throughout the neuron (Hama et al., 2004). In particular, in MEA experiments, Bis-I decreased the firing and bursting rates of rat neural networks *in vitro* (Robinette et al., 2011). Within the hNNF assay, Bis-I reliably reduced network parameters, e.g., burst duration, network burst percentage, and network synchronicity (AUNCC). Due to the enhanced variability of the mean firing rate, no significant effect of Bis-I was observed over all conducted experimental runs. Nevertheless, Bis-I is an appropriate endpoint-specific control for assessing neural network activity *in vitro*. As a negative control compound, acetaminophen showed no effect on network activity. A plethora of studies confirmed the use of acetaminophen as an apt negative control for DNT *in vitro* testing (Radio et al., 2008; Stern et al., 2014; Brown et al., 2016; Masjosthusmann et al., 2020). Nevertheless, a recently published study by Martin and colleagues categorized acetaminophen as an unfavorable negative control for DNT assays (Martin et al., 2022). This classification was made based on both clinical and preclinical reports, which indicate potential effects on the developing brain. Furthermore, the authors propose the use of low concentrations of acetaminophen ( $\leq 100 \mu\text{M}$ ) in recent DNT studies as a possible reason for the absence of compound-dependent effects. In comparison, chemicals like L-ascorbic acid, dinotefuran, and metformin were listed as “favorable” and should be included in a compound set for later determination of the assay’s general performance (Martin et al., 2022). Following the recommendations of Crofton and colleagues, a training set of chemicals should be designed and assayed (P9 “Training set chemicals”) after demonstrating that the test method has the aforementioned characteristics. Chemicals that produce a reliable effect on the endpoint in focus and chemicals that do not should be included, which allows both specificity and sensitivity of the assay to be determined (P11 “Specificity and sensitivity”). The hNNF assay was established and used within a research project with a focus on pesticides. Owing to the high cost involved in performing substance screening in the assay, it was not possible to distinguish between training and test set of chemicals during the establishment process. Instead, we selected pesticides that have a different DNT potential according to several *in vivo* and *in vitro* studies (P10 “Testing set chemicals”; Masjosthusmann et al., 2020). Pyrethroids, for example, are connected to neurodevelopmental disorders during childhood after pyrethroid pesticide exposure in epidemiological studies (Oulhote and Bouchard, 2013; Xue et al., 2013; Pitzer et al., 2021). Especially deltamethrin is a thoroughly studied type II pyrethroid, for which animal studies reported long-term effects on the brain (summa-



rized in Pitzer et al., 2021), which was also observed *in vitro* (Shafer et al., 2008; Masjosthusmann et al., 2020). In contrast, the neonicotinoid dinotefuran was described as DNT negative *in vivo* (Sheets et al., 2016) and also recommended as a negative tool compound for alternative DNT test methods (Aschner et al., 2017). In the future, the hNNF assay will be challenged with more chemicals that are well-described DNT positive and negative compounds to assess specificity and sensitivity of the assay and to enhance the readiness of the test method (Bal-Price et al., 2018). Currently, the academic setup of the hNNF assay allows parallel testing of 12 compounds ( $n = 1$ ) within the 35-day experimental period. However, it is possible to increase the throughput by increasing the plate size format from 48- to 96-well or by introducing automation. Duplicating the experimental set-up by using multiple MEA recording devices or by shifting the recording days in a periodic manner would also increase the throughput (P12 “High throughput”). Principle 13 (“Documentation”) highlights the importance of documenting the test method in detail to allow easy transfer and implementation across laboratories. A detailed standardized protocol exists and is currently being transferred to a laboratory of the U.S. EPA. After initial establishment of the assay in the collaborating laboratory, the hNNF assay will be challenged with a set of test substances to inform about the robustness and inter-laboratory transferability of the assay. This point is also emphasized in principle 14 (“Transferability”), along with the guaranteed availability of the cells used, which can be purchased commercially by other researchers. Currently, the generated data is not being shared through an open access databased (P15 “Data sharing”), but the authors aim to include hNNF data in a future ToxCast<sup>TM</sup><sup>4</sup> release.

In summary, the hNNF assay fulfils the majority of the principles proposed by Crofton et al. (2011) for the establishment of *in vitro* DNT assays for substance screening. Currently, the low number of tested chemicals defines the lack of readiness of the assay (Phase I Readiness Score B, Phase II Readiness Score C; Bal-Price et al., 2018), and the improvements required for the assay to be ready will be tackled in the future by testing known DNT positive substances (Aschner et al., 2017).

#### 4.2 The hNNF assay compared to its rat counterpart

The hNNF assay was established to model neural network formation and function in a human-based cell model and to become a valuable addition to the current DNT IVB, which comprises 17 different test methods able to measure changes in key neurodevelopmental processes (Masjosthusmann et al., 2020; Crofton and Mundy, 2021). Neural network formation and function is currently modelled in an assay based on rat primary cortical cells (rNNF), assessing the developmental effects of chemicals over 12 days of differentiation (Brown et al., 2016). It is important to mention that we aligned the hNNF assay with the parameter set of the rNNF assay, and thus both assays provide comparable parameters of network development (e.g.,

number of active electrodes or burst duration) to reduce uncertainty. Table 2 juxtaposes the results obtained in this study with rNNF data (Frank et al., 2017). Comparing the BMC<sub>50</sub> values of the most sensitive endpoint (MSE) between the hNNF and rNNF assay, it becomes clear that the observed positive hits differ in sensitivity across all substances. The rNNF seems to be more sensitive as it detects effects on network activity even at lower concentrations of the tested substances, e.g., deltamethrin (BMC<sub>50</sub> MSE hNNF: 2.74  $\mu$ M; BMC<sub>50</sub> MSE rNNF: 0.5  $\mu$ M). Aldicarb and chlorpyrifos were negative in the hNNF but altered network formation in the rNNF assay. Acetaminophen was tested negative in both assays.

The hNNF and rNNF are referred to as complementary assays because they measure similar endpoints, i.e., several MEA parameters, but differ with regard to species (rat vs. human), presence of fetal bovine serum (FBS), and assay technology (beginning and washout of compounds before MEA recordings). Therefore, differences in data obtained within these assays are not necessarily evidence of a false detection (Crofton and Mundy, 2021). These differences may result from several differences in the assay setup, i.e., species differences and exposure schemes. The hNNF and rNNF assays are based on the same basic cell types, namely neurons and astrocytes, but derived from different species (hNNF: human iPSC-derived neurons and primary astroglia; rNNF: rat primary neocortical cells). It is widely accepted that the predictability of non-human-based assays for human health is limited by species differences (Leist and Hartung, 2013). Also, primary neural progenitor cells (NPC) derived from rats (PND5) are more sensitive towards exposure to DNT compounds compared to time-matched primary human NPCs *in vitro* (Baumann et al., 2016). These two systems differ not only in their sensitivity but also with regard to their molecular equipment notwithstanding similar cellular functions (e.g., NPC migration and differentiation; Masjosthusmann et al., 2018). Recently, the co-culture system applied in this study was used for comparing acute effects of neurotoxic compounds on network activity to rodent cultures (rNNF) and revealed a considerable delay in human iPSC-derived neuronal and glial co-culture compared to rat cortical cultures (Saavedra et al., 2021). In general, the developing rat brain exhibits some crucial differences to human brain development *in vivo*, such as the absence of gyration, which adds complexity to the human brain (Dubois et al., 2008). Furthermore, it has been demonstrated that embryonic day (E) 18 and E21 during rat brain development match week 8-9 and week 15-16 after fertilization in human embryo, when looking at neurogenesis (Bayer et al., 1993). The faster maturation of rodent cells compared to human cells *in vitro* was also suggested by Masjosthusmann et al. (2018).

As the compound set presented in Table 2 is rather small and focused on pesticides, we cannot draw general conclusions about species-specific differences in sensitivity between the rNNF and hNNF assays. As suggested by Baumann et al. (2016), testing of additional compounds with known MoAs is required to infer

<sup>4</sup> <http://www.epa.gov/ncct/toxcast>



**Tab. 2: Comparison of BMC<sub>50</sub> values of the most sensitive endpoint (MSE) for chemicals (same CASRN) tested in the hNNF (this study) and rNNF assay (Frank et al., 2017)**

↑ indicates an inductive effect (BMC<sub>50</sub>ind).

	Acetaminophen	Aldicarb	Carbaryl	Chlorpyrifos	Deltamethrin	Fipronil	Imidacloprid
BMC <sub>50</sub> MSE hNNF	no hit	no hit	17.31↑	no hit	2.74	11.48 ↑	15.51
BMC <sub>50</sub> MSE rNNF	no hit	0.66	0.08	1.4	0.5	1.33	9.99

more general species-specific sensitivity. Nevertheless, our data highlights the importance of considering species specificities when comparing screening results.

Besides the species, experimental procedures differ between the human and rat NNF assays and may also lead to differences in assay sensitivity. Two major exposure differences are crucial. First, the time point when the compound is administered differs between the hNNF and rNNF assay. Rat cortical cultures are exposed to the compound two hours after seeding the cells on MEAs, whereas the first day of dosing in hNNF experiments is DIV 7, when first single spike activities are visible. The respective networks are at different stages of development at this time, i.e., in contrast to human cells, rat cortical cells are barely established in the culture dish. Not yet established cells challenged shortly after the plating process may be more susceptible to substance exposure than networks that have already been able to differentiate for a week in chemical-free medium. In the rNNF assay, early processes like neurite initiation and outgrowth as well as glial proliferation are potentially disrupted within the first 24 h (Harrill et al., 2011; Frank et al., 2017), whereas these processes can proceed undisturbed during the first seven days of differentiation and contribute to network development in the hNNF assay. Both assays thus depict different stages of neural network development and hence include different windows of neurodevelopmental processes. In addition, the hNNF culture medium, in contrast to the rNNF medium, is supplemented with FBS, which contains a variety of plasma proteins, peptides, and growth factors. Recent studies have shown that FBS in cell culture medium attenuates the toxicity caused by specific compounds due to their high affinity for binding to proteins, which then results in higher BMC values (Zhang, Y. et al., 2016; Zhang, R., 2020). The influence of FBS on the human cultures with regards to network effects needs to be studied by assessment of *in vitro* kinetics in the future (Kramer et al., 2015). Secondly, the washout of the respective compound 24 h prior to the recording is a unique feature of the hNNF assay and aims at minimizing acute substance effects during MEA recordings. There is evidence that specific substances directly target synaptic receptors and acutely affect brain function. For example, the NMDAR is a prime target of the heavy metal lead, leading to the inhibition of glutamatergic synapse activity (Toscano and Guilarate, 2005). To diminish the measurement of these acute effects and to only assess the effects of substances on neural network development, we introduced washout steps into the experimental procedure of the hNNF. In comparison to the rNNF results (Tab. 2), it is possible that the presence of compounds during

MEA measurements contributes to higher sensitivity of the rat versus the human NNF assay.

All of the aforementioned variations in assay setup and biology, either alone or in combination, can explain the discrepancies in sensitivity between the two test methods. In the future, exposure schemes of the two NNF assays should be harmonized in order to understand the true nature of species differences concerning neural network formation. This might substantially help to extrapolate from rat *in vivo* studies to humans using the parallelogram approach (Baumann et al., 2016).

#### 4.3 Use of hNNF data on deltamethrin for the development of a putative AOP

In 2021, the EFSA developed an IATA case study with the goal of including all available *in vivo* and *in vitro* data, among others the data generated within the DNT IVB for DNT hazard identification for the Type II pyrethroid insecticide deltamethrin (Crofton and Mundy, 2021; Hernández-Jerez et al., 2021). Epidemiological studies revealed associations between childhood exposure to pyrethroids like deltamethrin and neurodevelopmental disorders, e.g., attention deficit hyperactivity disorder or autism spectrum disorder (Oulhote and Bouchard, 2013; Shelton et al., 2014; Wagner-Schuman et al., 2015). As previously shown, deltamethrin negatively influenced 5 of 14 parameters describing network function with “Number of spikes per network burst” as the most sensitive endpoint within the hNNF assay (BMC<sub>50</sub> 2.7 µM). Here, interference with voltage-gated sodium channels is the most commonly known MoA for pyrethroid insecticides like deltamethrin (Tapia et al., 2020), representing one of two molecular initiating events (MIE) within the stressor-specific AOP network (Fig. 7). This MIE is followed by key events 1-6 and 9, describing different cellular responses, like the disruption of sodium channel gate kinetics leading to disruption of action potential, that in the end cumulate in an impaired behavioral function (adverse outcome). KE4 describes the alteration of neural network function as shown also by data assessed in the rNNF (BMC<sub>50</sub> 0.5 µM; Tab. 2) and hNNF assay. The 5-fold higher BMC of the hNNF assay compared to the rNNF assay might be explained by the different exposure paradigm and/or the different species as discussed above in more detail. Furthermore, potential mechanisms or processes that are disrupted by a chemical agent can be revealed and used for the development of adverse outcome pathways (AOP) and also set a new focus for more hypothesis-driven *in vivo* studies (Hernández-Jerez et al., 2021). The postulated stressor-based AOP network (Fig. 7) is currently not included in the OECD AOP Wiki, but the EFSA

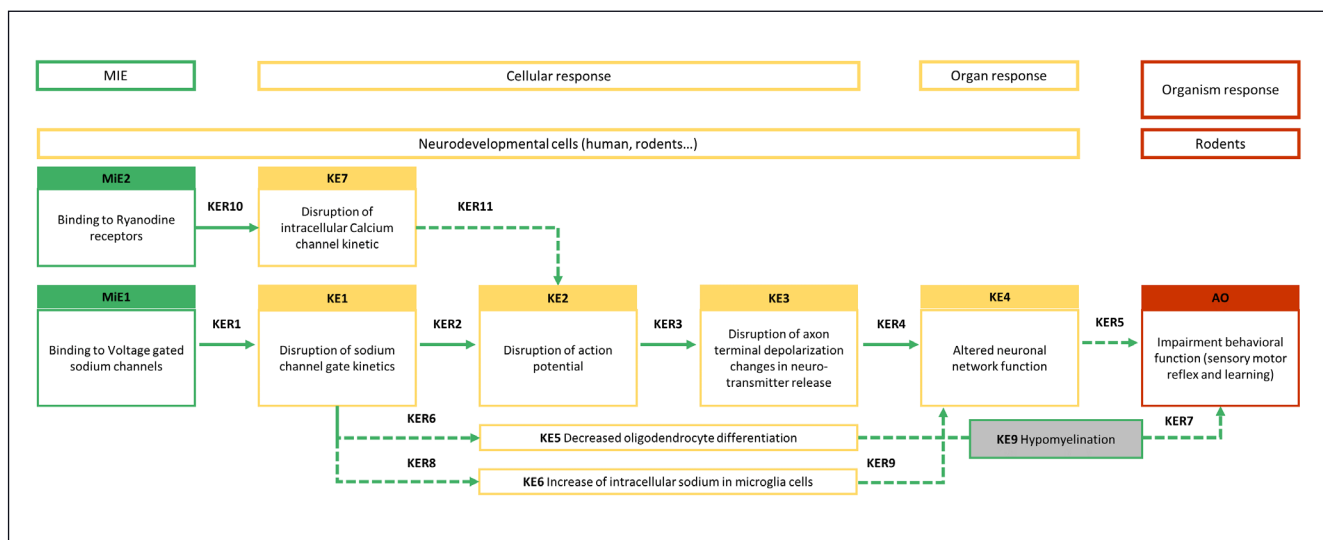


**Fig. 7: AOP network on deltamethrin postulated by the EFSA Panel on Plant Protection Products and their Residues**

Non-adjacent key events for which the biological reasonability and/or empirical evidence is less assured are marked by dashed lines. MIE, molecular initiating event; KE, key event; KER, key event relationship; AO, adverse outcome. Adapted from Hernández-Jerez et al. (2021).

Panel on Plant Protection Products and their Residues recommends its submission to the OECD program to further support a regulatory uptake. This case study and the inclusion of hNNF data on deltamethrin exposure showed the applicability of the hNNF assay for hazard identification and characterization, consistent with the other assays of the DNT IVB.

The presented study provides insight into the establishment of a novel new approach method assessing alterations on neural network formation and function using an hiPSC-derived co-culture of neurons and primary astroglia. The cell model comprises a broad variety of genes expressed exclusively in neurons and astrocytes as a prerequisite for neural network function after the GABA switch. For example, together with the rNNF assay, it is capable of representing NMDAR expression and assessing any MoA involving NMDAR, which distinguishes these NNF assays from other assays of the DNT IVB (Masjosthusmann et al., 2020). Compared to other studies using excitatory and inhibitory iNs, the hNNF performs similarly with regard to, e.g., firing rates and number of active electrodes. For example, Saavedra and colleagues cultured the excitatory and inhibitory iNS, which resulted in 14 to 16 active electrodes after 37 days and a mean firing rate between 1 and 2 Hz after 21 days. Furthermore, the described test system was successfully used to assess acute neuroactive effects of chemicals (Saavedra et al., 2021; Tukker et al., 2020a,b). Although multiple labs utilize MEAs for assessing acute effects on neural network activity, the number of publications dealing with the effects of pesticides on electrophysiological endpoints for DNT using human cells is very limited (Di Consiglio et al., 2020; Pistollato et al., 2021).

Besides astrocytes, also other cell types play an important role in development and function of neural networks, such as oligodendrocytes, responsible for myelination (Doretto et al., 2011), or microglia, which, among other things, phagocytose weak syn-

apses and regulate neurogenesis (Miyamoto et al., 2016; Paolucci and Ferretti, 2017). To represent all processes appropriately, the hNNF assay must be complemented with the missing cell types. Still, a proactive establishment of the assay already reached a medium readiness for use in regulatory screening approaches with possible improvements in type and number of test method controls, inter- and intra-lab transferability, and definition of the applicability domains. The testing of 28 substances revealed the suitability of the assay for screening environmental chemicals like pesticides. In the future, the throughput of the hNNF assay as well as its robustness and specificity will be increased by testing additional substances, thereby enlarging the chemical space, to present a suitable addition to the current DNT IVB and close one of the identified gaps regarding network formation and function.

## References

- Aschner, M., Ceccatelli, S., Daneshian, M. et al. (2017). Reference compounds for alternative test methods to indicate developmental neurotoxicity (DNT) potential of chemicals: Example lists and criteria for their selection and use. *ALTEX 34*, 49-74. doi:10.14573/altex.1604201
- Bal-Price, A., Crofton, K. M., Leist, M. et al. (2015). International STakeholder NETwork (ISTNET): Creating a developmental neurotoxicity (DNT) testing road map for regulatory purposes. *Arch Toxicol 89*, 269-287. doi:10.1007/S00204-015-1464-2
- Bal-Price, A., Hogberg, H. T., Crofton, K. M. et al. (2018). Recommendation on test readiness criteria for new approach methods in toxicology: Exemplified for developmental neurotoxicity. *ALTEX 35*, 306-352. doi:10.14573/altex.1712081
- Bartmann, K., Hartmann, J., Kapr, J. et al. (2021). Measurement of electrical activity of differentiated human iPSC-derived



- neurospheres recorded by microelectrode arrays (MEA). In J. Llorens and M. Barenys (eds), *Experimental Neurotoxicology Methods* (473-488). Neuromethods 172. New York: Humana. doi:10.1007/978-1-0716-1637-6\_22
- Baumann, J., Barenys, M., Gassmann, K. et al. (2014). Comparative human and rat “neurosphere assay” for developmental neurotoxicity testing. *Curr Protoc Toxicol* 59, 12.21.1-12.21.24. doi:10.1002/0471140856.TX1221S59
- Baumann, J., Dach, K., Barenys, M. et al. (2015). Application of the neurosphere assay for DNT hazard assessment: Challenges and limitations. In *Methods in Pharmacology and Toxicology* (29). Totowa, NJ: Humana Press. doi:10.1007/7653\_2015\_49
- Baumann, J., Gassmann, K., Masjosthusmann, S. et al. (2016). Comparative human and rat neurospheres reveal species differences in chemical effects on neurodevelopmental key events. *Arch Toxicol* 90, 1415-1427. doi:10.1007/S00204-015-1568-8
- Bayer, S. A., Altman, J., Russo, R. J. et al. (1993). Timetables of neurogenesis in the human brain based on experimentally determined patterns in the rat. *Neurotoxicology* 14, 83-144.
- Bennett, D., Bellinger, D. C., Birnbaum, L. S. et al. (2016). Project TENDR: Targeting environmental neuro-developmental risks the TENDR consensus statement. *Environ Health Perspect* 124, A118-A122. doi:10.1289/EHP358
- Bjørling-Poulsen, M., Andersen, H. R. and Grandjean, P. (2008). Potential developmental neurotoxicity of pesticides used in Europe. *Environ Health* 7, 50. doi:10.1186/1476-069X-7-50
- Blum, J., Masjosthusmann, S., Bartmann, K. et al. (2022). Establishment of a human cell-based in vitro battery to assess developmental neurotoxicity hazard of chemicals. *Chemosphere* 311, 137035. doi:10.1016/J.chemosphere.2022.137035
- Brown, J. P., Hall, D., Frank, C. L. et al. (2016). Evaluation of a microelectrode array-based assay for neural network ontogeny using training set chemicals. *Toxicol Sci* 154, 126-139. doi:10.1093/toxsci/kfw147
- Carstens, K. E., Carpenter, A. F., Martin, M. M. et al. (2022). Integrating data from in vitro new approach methodologies for developmental neurotoxicity. *Toxicol Sci* 187, 62-79. doi:10.1093/toxsci/kfac018
- Coecke, S., Goldberg, A. M., Allen, S. et al. (2007). Workgroup report: Incorporating in vitro alternative methods for developmental neurotoxicity into international hazard and risk assessment strategies. *Environ Health Perspect* 115, 924-931. doi:10.1289/ehp.9427
- Crofton, K. M., Mundy, W. R., Lein, P. J. et al. (2011). Developmental neurotoxicity testing: Recommendations for developing alternative methods for the screening and prioritization of chemicals. *ALTEX* 28, 9-15. doi:10.14573/altex.2011.1.009
- Crofton, K. M., Mundy, W. R. and Shafer, T. J. (2012). Developmental neurotoxicity testing: A path forward. *Congenit Anom* 52, 140-146. doi:10.1111/j.1741-4520.2012.00377.x
- Crofton, K., Fritzsche, E., Ylikomi, T. et al. (2014). International Stakeholder NETwork (ISTNET) for creating a developmental neurotoxicity testing (DNT) roadmap for regulatory purposes. *ALTEX* 31, 223-224. doi:10.14573/altex.1402121
- Crofton, K. M. and Mundy, W. R. (2021). External scientific report on the interpretation of data from the developmental neurotoxicity in vitro testing assays for use in integrated approaches for testing and assessment. *EFSA Support Publ* 18, 6924E. doi:10.2903/sp.efsa.2021.en-6924
- Dach, K., Bendt, F., Huebenthal, U. et al. (2017). BDE-99 impairs differentiation of human and mouse NPCs into the oligodendroglial lineage by species-specific modes of action. *Sci Rep* 7, 44861. doi:10.1038/srep44861
- Das, K. P., Freudenberg, T. M. and Mundy, W. R. (2004). Assessment of PC12 cell differentiation and neurite growth: A comparison of morphological and neurochemical measures. *Neurotoxicol Teratol* 26, 397-406. doi:10.1016/j.ntt.2004.02.006
- Di Consiglio, E., Pistollato, F., Mendoza-De Gyves, E. et al. (2020). Integrating biokinetics and in vitro studies to evaluate developmental neurotoxicity induced by chlorpyrifos in human iPSC-derived neural stem cells undergoing differentiation towards neuronal and glial cells. *Reprod Toxicol* 98, 174-188. doi:10.1016/j.reprotox.2020.09.010
- Doretto, S., Malerba, M., Ramos, M. et al. (2011). Oligodendrocytes as regulators of neuronal networks during early postnatal development. *PLoS One* 6, 19849. doi:10.1371/journal.pone.0019849
- Druwe, I., Freudenberg, T. M., Wallace, K. et al. (2015). Sensitivity of neuroprogenitor cells to chemical-induced apoptosis using a multiplexed assay suitable for high-throughput screening. *Toxicology* 333, 14-24. doi:10.1016/J.TOX.2015.03.011
- Druwe, I., Freudenberg, T. M., Wallace, K. et al. (2016). Comparison of human induced pluripotent stem cell-derived neurons and rat primary cortical neurons as in vitro models of neurite outgrowth. *Appl Vitr Toxicol* 2, 26-36. doi:10.1089/avt.2015.0025
- Dubois, J., Binders, M., Borradori-Tolsa, C. et al. (2008). Primary cortical folding in the human newborn: An early marker of later functional development. *Brain* 131, 2028-2041. doi:10.1093/brain/awn137
- EFSA (2013). Scientific Opinion on the developmental neurotoxicity potential of acetamiprid and imidacloprid. *EFSA J* 11, 3471. doi:10.2903/j.efsa.2013.3471
- Frank, C. L., Brown, J. P., Wallace, K. et al. (2017). Developmental neurotoxicants disrupt activity in cortical networks on microelectrode arrays: Results of screening 86 compounds during neural network formation. *Toxicol Sci* 160, 121-135. doi:10.1093/toxsci/kfx169
- Fritzsche, E., Alm, H., Baumann, J. et al. (2015). Literature review on in vitro and alternative developmental neurotoxicity (DNT) testing methods. *EFSA Support Publ* 12, 778E. doi:10.2903/sp.efsa.2015.en-778
- Fritzsche, E. (2017). Report on Integrated Testing Strategies for the identification and evaluation of chemical hazards associated with the developmental neurotoxicity (DNT), to facilitate discussions at the Joint EFSA/OECD Workshop on DNT. *EFSA Support Publ* 14, 1191E. doi:10.2903/sp.efsa.2017.en-1191
- Fritzsche, E., Crofton, K. M., Hernandez, A. F. et al. (2017). OECD/EFSA workshop on developmental neurotoxicity (DNT): The use of non-animal test methods for regulatory purposes. *ALTEX* 34, 311-315. doi:10.14573/altex.1701171
- Fritzsche, E., Barenys, M., Klose, J. et al. (2018a). Current availability of stem cell-based in vitro methods for developmental neu-



- rotoxicity (DNT) testing. *Toxicol Sci* 165, 21-30. doi:10.1093/toxsci/kfy178
- Fritzsche, E., Grandjean, P., Crofton, K. M. et al. (2018b). Consensus statement on the need for innovation, transition and implementation of developmental neurotoxicity (DNT) testing for regulatory purposes. *Toxicol Appl Pharmacol* 354, 3-6. doi:10.1016/J.TAAP.2018.02.004
- Glantz, L. A., Gilmore, J. H., Hamer, R. M. et al. (2007). Synaptophysin and PSD-95 in the human prefrontal cortex from mid-gestation into early adulthood. *Neuroscience* 149, 582-591. doi:10.1016/j.neuroscience.2007.06.036
- Goldman, L. R. and Koduru, S. (2000). Chemicals in the environment and developmental toxicity to children: A public health and policy perspective. *Environ Health Perspect* 108, 443-448. doi:10.1289/EHP.00108S3443
- Grandjean, P. and Landrigan, P. (2006). Developmental neurotoxicity of industrial chemicals. *Lancet* 368, 2167-2178. doi:10.1016/S0140-6736(06)69665-7
- Hama, H., Hara, C., Yamaguchi, K. et al. (2004). PKC signaling mediates global enhancement of excitatory synaptogenesis in neurons triggered by local contact with astrocytes. *Neuron* 41, 405-415. doi:10.1016/S0896-6273(04)00007-8
- Hardy, A., Benford, D., Halldorsson, T. et al. (2017). Guidance on the use of the weight of evidence approach in scientific assessments. *EFSA J* 15, e04971. doi:10.2903/j.efsa.2017.4971
- Harrill, J. A., Freudenrich, T. M., Machacek, D. W. et al. (2010). Quantitative assessment of neurite outgrowth in human embryonic stem cell-derived hN2 cells using automated high-content image analysis. *Neurotoxicology* 31, 277-290. doi:10.1016/j.neuro.2010.02.003
- Harrill, J. A., Robinette, B. L. and Mundy, W. R. (2011). Use of high content image analysis to detect chemical-induced changes in synaptogenesis in vitro. *Toxicol In Vitro* 25, 368-387. doi:10.1016/j.tiv.2010.10.011
- Harrill, J. A., Robinette, B. L., Freudenrich, T. et al. (2013). Use of high content image analyses to detect chemical-mediated effects on neurite sub-populations in primary rat cortical neurons. *Neurotoxicology* 34, 61-73. doi:10.1016/j.neuro.2012.10.013
- Harrill, J. A., Freudenrich, T., Wallace, K. et al. (2018). Testing for developmental neurotoxicity using a battery of in vitro assays for key cellular events in neurodevelopment. *Toxicol Appl Pharmacol* 354, 24-39. doi:10.1016/J.TAAP.2018.04.001
- Hernández-Jerez, A., Adriaanse, P., Aldrich, A. et al. (2021). Development of Integrated Approaches to Testing and Assessment (IATA) case studies on developmental neurotoxicity (DNT) risk assessment. *EFSA J* 19, e06599. doi:10.2903/j.efsa.2021.6599
- Hoelting, L., Klima, S., Karreman, C. et al. (2016). Stem cell-derived immature human dorsal root ganglia neurons to identify peripheral neurotoxicants. *Stem Cells Transl Med* 5, 476-487. doi:10.5966/SCTM.2015-0108
- Hofrichter, M., Nimtz, L., Tigges, J. et al. (2017). Comparative performance analysis of human iPSC-derived and primary neural progenitor cells (NPC) grown as neurospheres in vitro. *Stem Cell Res* 25, 72-82. doi:10.1016/J.SCR.2017.10.013
- Holst, C. B., Brøchner, C. B., Vitting-Seerup, K. et al. (2019). Astrogenesis in human fetal brain: Complex spatiotemporal im-
- munoreactivity patterns of GFAP, S100, AQP4 and YKL-40. *J Anat* 235, 590-615. doi:10.1111/JOA.12948
- Hyvärinen, T., Hyysalo, A., Kapucu, F. E. et al. (2019). Functional characterization of human pluripotent stem cell-derived cortical networks differentiated on laminin-521 substrate: Comparison to rat cortical cultures. *Sci Rep* 9, 17125. doi:10.1038/s41598-019-53647-8
- Ishii, M. N., Yamamoto, K., Shoji, M. et al. (2017). Human induced pluripotent stem cell (hiPSC)-derived neurons respond to convulsant drugs when co-cultured with hiPSC-derived astrocytes. *Toxicology* 389, 130-138. doi:10.1016/j.tox.2017.06.010
- Johnstone, A. F. M., Gross, G. W., Weiss, D. G. et al. (2010). Microelectrode arrays: A physiologically based neurotoxicity testing platform for the 21<sup>st</sup> century. *Neurotoxicology* 31, 331-350. doi:10.1016/j.neuro.2010.04.001
- Johnston, G. A. R. (2013). Advantages of an antagonist: Bicuculline and other GABA antagonists. *Br J Pharmacol* 169, 328-336. doi:10.1111/BPH.12127
- Karlin, A. (2002). Emerging structure of the nicotinic acetylcholine receptors. *Nat Rev Neurosci* 3, 102-114. doi:10.1038/nrn731
- Klose, J., Tigges, J., Masjosthusmann, S. et al. (2021). TBBPA targets converging key events of human oligodendrocyte development resulting in two novel AOPs. *ALTEX* 38, 215-234. doi:10.14573/altex.2007201
- Koch, K., Bartmann, K., Hartmann, J. et al. (2022). Scientific validation of human neurosphere assays for developmental neurotoxicity evaluation. *Front Toxicol* 4, 816370. doi:10.3389/ftox.2022.816370
- Kosnik, M. B., Strickland, J. D., Marvel, S. W. et al. (2020). Concentration-response evaluation of ToxCast compounds for multivariate activity patterns of neural network function. *Arch Toxicol* 94, 469-484. doi:10.1007/s00204-019-02636-x
- Kramer, N. I., Di Consiglio, E., Blaabuwer, B. J. et al. (2015). Bio-kinetics in repeated-dosing in vitro drug toxicity studies. *Toxicol In Vitro* 30, 217-224. doi:10.1016/j.tiv.2015.09.005
- Krug, A. K., Balmer, N. V., Matt, F. et al. (2013). Evaluation of a human neurite growth assay as specific screen for developmental neurotoxicants. *Arch Toxicol* 87, 2215-2231. doi:10.1007/s00204-013-1072-y
- Kuehn, B. M. (2010). Increased risk of ADHD associated with early exposure to pesticides, PCBs. *JAMA* 304, 27-28. doi:10.1001/jama.2010.860
- Leist, M. and Hartung, T. (2013). Reprint: Inflammatory findings on species extrapolations: Humans are definitely no 70-kg mice. *ALTEX* 30, 227-230. doi:10.14573/altex.2013.2.227
- Leonzino, M., Busnelli, M., Antonucci, F. et al. (2016). The timing of the excitatory-to-inhibitory GABA switch is regulated by the oxytocin receptor via KCC2. *Cell Rep* 15, 96-103. doi:10.1016/j.celrep.2016.03.013
- Little, D., Ketteler, R., Gissen, P. et al. (2019). Using stem cell-derived neurons in drug screening for neurological diseases. *Neurobiol Aging* 78, 130-141. doi:10.1016/j.neurobiolaging.2019.02.008
- Maccioni, R. B. and Cambiazo, V. (1995). Role of microtubule-associated proteins in the control of microtubule assembly. *Phys Rev* 75, 835-864. doi:10.1152/physrev.1995.75.4.835



- Macdonald, R. L., Rogers, C. J. and Twyman, R. E. (1989). Kinetic properties of the GABA receptor main conductance state of mouse spinal cord neurones in culture. *J Physiol* 410, 479-499. doi:10.1113/jphysiol.1989.sp017545
- Mack, C. M., Lin, B. J., Turner, J. D. et al. (2014). Burst and principal components analyses of MEA data for 16 chemicals describe at least three effects classes. *Neurotoxicology* 40, 75-85. doi:10.1016/j.neuro.2013.11.008
- Martin, M. M., Baker, N. C., Boyes, W. K. et al. (2022). An expert-driven literature review of “negative” chemicals for developmental neurotoxicity (DNT) in vitro assay evaluation. *Neurotoxicol Teratol* 93, 107117. doi:10.1016/j.ntt.2022.107117
- Masjosthusmann, S., Becker, D., Petzuch, B. et al. (2018). A transcriptome comparison of time-matched developing human, mouse and rat neural progenitor cells reveals human uniqueness. *Toxicol Appl Pharmacol* 354, 40-55. doi:10.1016/j.taap.2018.05.009
- Masjosthusmann, S., Blum, J., Bartmann, K. et al. (2020). Establishment of an a priori protocol for the implementation and interpretation of an in-vitro testing battery for the assessment of developmental neurotoxicity. *EFSA Support Publ* 17, 1938E. doi:10.2903/sp.efsa.2020.en-1938
- Missale, C., Nash, S. R., Robinson, S. W. et al. (1998). Dopamine receptors: From structure to function. *Physiol Rev* 78, 189-225. doi:10.1152/physrev.1998.78.1.189
- Miyamoto, A., Wake, H., Ishikawa, A. W. et al. (2016). Microglia contact induces synapse formation in developing somatosensory cortex. *Nat Commun* 7, 12540. doi:10.1038/ncomms12540
- Neuman, R. S., Ben-Ari, Y., Gho, M. et al. (1988). Blockade of excitatory synaptic transmission by 6-cyano-7-nitroquinoxaline-2,3-dione (CNQX) in the hippocampus in vitro. *Neurosci Lett* 92, 64-68. doi:10.1016/0304-3940(88)90743-4
- Nimtz, L., Klose, J., Masjosthusmann, S. et al. (2019). The neurosphere assay as an in vitro method for developmental neurotoxicity (DNT) evaluation. *Neuromethods* 145, 141-168. doi:10.1007/978-1-4939-9228-7\_8
- Nimtz, L., Hartmann, J., Tigges, J. et al. (2020). Characterization and application of electrically active neuronal networks established from human induced pluripotent stem cell-derived neural progenitor cells for neurotoxicity evaluation. *Stem Cell Res* 45, 101761. doi:10.1016/j.scr.2020.101761
- NRC – National Research Council (2000). *Scientific Frontiers in Developmental Toxicology and Risk Assessment*. National Academies Press. doi:10.17226/9871
- Nyffeler, J., Dolde, X., Krebs, A. et al. (2017). Combination of multiple neural crest migration assays to identify environmental toxicants from a proof-of-concept chemical library. *Arch Toxicol* 91, 3613-3632. doi:10.1007/s00204-017-1977-y
- Ockleford, C., Adriaanse, P., Hougaard Bennekou, S. et al. (2018). Scientific opinion on pesticides in foods for infants and young children. *EFSA J* 16, e05286. doi:10.2903/j.efsa.2018.5286
- Odawara, A., Katoh, H., Matsuda, N. et al. (2016). Physiological maturation and drug responses of human induced pluripotent stem cell-derived cortical neuronal networks in long-term culture. *Sci Rep* 6, 26181. doi:10.1038/srep26181
- Odawara, A., Matsuda, N., Ishibashi, Y. et al. (2018). Toxicological evaluation of convulsant and anticonvulsant drugs in human induced pluripotent stem cell-derived cortical neuronal networks using an MEA system. *Sci Rep* 8, 10416. doi:10.1038/s41598-018-28835-7
- OECD (2007). Test No. 426: Developmental Neurotoxicity Study. *OECD Guidelines for the Testing of Chemicals, Section 4: Health Effects*. <http://www.oecd.org/dataoecd/20/52/37622194.pdf> (accessed 22.07.2021)
- Okado, N., Kakimi, S. and Kojima, T. (1979). Synaptogenesis in the cervical cord of the human embryo: Sequence of synapse formation in a spinal reflex pathway. *J Comp Neurol* 184, 491-517. doi:10.1002/cne.901840305
- Oulhote, Y. and Bouchard, M. F. (2013). Urinary metabolites of organophosphate and pyrethroid pesticides and behavioral problems in Canadian children. *Environ Health Perspect* 121, 1378-1384. doi:10.1289/ehp.1306667
- Paolicelli, R. C. and Ferretti, M. T. (2017). Function and dysfunction of microglia during brain development: Consequences for synapses and neural circuits. *Front Synaptic Neurosci* 9, 9. doi:10.3389/fnsyn.2017.00009
- Paparella, M., Bennekou, S. H. and Bal-Price, A. (2020). An analysis of the limitations and uncertainties of in vivo developmental neurotoxicity testing and assessment to identify the potential for alternative approaches. *Reprod Toxicol* 96, 327-336. doi:10.1016/j.reprotox.2020.08.002
- Pistollato, F., Carpi, D., Mendoza-de Gyves, E. et al. (2021). Combining in vitro assays and mathematical modelling to study developmental neurotoxicity induced by chemical mixtures. *Reprod Toxicol* 105, 101-119. doi:10.1016/j.reprotox.2021.08.007
- Pitzer, E. M., Williams, M. T. and Vorhees, C. V. (2021). Effects of pyrethroids on brain development and behavior: Deltamethrin. *Neurotoxicol Teratol* 87, 106983. doi:10.1016/j.ntt.2021.106983
- Radio, N. M., Breier, J. M., Shafer, T. J. et al. (2008). Assessment of chemical effects on neurite outgrowth in PC12 cells using high content screening. *Toxicol Sci* 105, 106-118. doi:10.1093/toxsci/kfn114
- Robinette, B. L., Harrill, J. A., Mundy, W. R. et al. (2011). In vitro assessment of developmental neurotoxicity: Use of microelectrode arrays to measure functional changes in neuronal network ontogeny. *Front Neuroeng* 4, 1-9. doi:10.3389/fneng.2011.00001
- Rodier, P. M. (1995). Developing brain as a target of toxicity. *Environ Health Perspect* 103, Suppl 6, 73-76. doi:10.1289/ehp.95103s673
- Saavedra, L., Wallace, K., Freudenberg, T. F. et al. (2021). Comparison of acute effects of neurotoxic compounds on network activity in human and rodent neural cultures. *Toxicol Sci* 180, 295-312. doi:10.1093/toxsci/kfab008
- Sachana, M., Bal-Price, A., Crofton, K. M. et al. (2019). International regulatory and scientific effort for improved developmental neurotoxicity testing. *Toxicol Sci* 167, 45-57. doi:10.1093/toxsci/kfy211
- Sagiv, S. K., Thurston, S. W., Bellinger, D. C. et al. (2010). Prenatal organochlorine exposure and behaviors associated with attention deficit hyperactivity disorder in school-aged children. *Am J Epidemiol* 171, 593-601. doi:10.1093/aje/kwp427
- Schmuck, M. R., Temme, T., Dach, K. et al. (2017). Omnisphero:



- A high-content image analysis (HCA) approach for phenotypic developmental neurotoxicity (DNT) screenings of organoid neurosphere cultures *in vitro*. *Arch Toxicol* 91, 2017-2028. doi:10.1007/s00204-016-1852-2
- Seki, T. (2002). Expression patterns of immature neuronal markers PSA-NCAM, CRMP-4 and NeuroD in the hippocampus of young adult and aged rodents. *J Neurosci Res* 70, 327-334. doi:10.1002/jnr.10387
- Shafer, T. J., Rijal, S. O. and Gross, G. W. (2008). Complete inhibition of spontaneous activity in neuronal networks *in vitro* by deltamethrin and permethrin. *Neurotoxicology* 29, 203-212. doi:10.1016/j.neuro.2008.01.002
- Shafer, T. J. (2019). Application of microelectrode array approaches to neurotoxicity testing and screening. *Adv Neurobiol* 22, 275-297. doi:10.1007/978-3-030-11135-9\_12
- Sheets, L. P., Li, A. A., Minnema, D. J. et al. (2016). A critical review of neonicotinoid insecticides for developmental neurotoxicity. *Crit Rev Toxicol* 46, 153-190. doi:10.3109/10408444.2015.1090948
- Shelton, J. F., Geraghty, E. M., Tancredi, D. J. et al. (2014). Neurodevelopmental disorders and prenatal residential proximity to agricultural pesticides: The charge study. *Environ Health Perspect* 122, 1103-1109. doi:10.1289/ehp.1307044
- Smirnova, L., Hogberg, H. T., Leist, M. et al. (2014). Food for thought ... Developmental neurotoxicity – Challenges in the 21<sup>st</sup> century and *in vitro* opportunities. *ALTEX* 31, 129-156. doi:10.14573/altex.1403271
- Stern, M., Gierse, A., Tan, S. et al. (2014). Human Ntera2 cells as a predictive *in vitro* test system for developmental neurotoxicity. *Arch Toxicol* 88, 127-136. doi:10.1007/S00204-013-1098-1
- Takahashi, K., Tanabe, K., Ohnuki, M. et al. (2007). Induction of pluripotent stem cells from adult human fibroblasts by defined factors. *Cell* 131, 861-872. doi:10.1016/j.cell.2007.11.019
- Tapia, C. M., Folorunso, O., Singh, A. K. et al. (2020). Effects of deltamethrin acute exposure on Nav1.6 channels and medium spiny neurons of the nucleus accumbens. *Toxicology* 440, 152488. doi:10.1016/j.tox.2020.152488
- Terron, A. and Bennekou, S. H. (2018). Towards a regulatory use of alternative developmental neurotoxicity testing (DNT). *Toxicol Appl Pharmacol* 354, 19-23. doi:10.1016/j.taap.2018.02.002
- Toscano, C. D. and Guilarte, T. R. (2005). Lead neurotoxicity: From exposure to molecular effects. *Brain Res Rev* 49, 529-554. doi:10.1016/j.brainresrev.2005.02.004
- Tsuji, R. and Crofton, K. M. (2012). Developmental neurotoxicity guideline study: Issues with methodology, evaluation and regulation\*. *Congenit Anom (Kyoto)* 52, 122-128. doi:10.1111/J.1741-4520.2012.00374.X
- Tukker, A. M., Bouwman, L. M. S., van Kleef, R. G. D. M. et al. (2020a). Perfluoroctane sulfonate (PFOS) and perfluorooctanoate (PFOA) acutely affect human  $\alpha 1\beta 2\gamma 2L$  GABAA receptor and spontaneous neuronal network function *in vitro*. *Sci Rep* 10, 5311. doi:10.1038/s41598-020-62152-2
- Tukker, A. M., Wijnolts, F. M. J., de Groot, A. et al. (2020b). Applicability of hiPSC-derived neuronal co-cultures and rodent primary cortical cultures for *in vitro* seizure liability assessment. *Toxicol Sci* 178, 71-87. doi:10.1093/toxsci/kfaa136
- Uhlhaas, P. and Singer, W. (2006). Neural synchrony in brain disorders: Relevance for cognitive dysfunctions and pathophysiology. *Neuron* 52, 155-168. doi:10.1016/j.neuron.2006.09.020
- U.S. EPA (1998). Health Effects Guidelines OPPTS 870.6300. *Dev Neurotox Study EPA* 71.
- Wagner-Schuman, M., Richardson, J. R., Auinger, P. et al. (2015). Association of pyrethroid pesticide exposure with attention-deficit/hyperactivity disorder in a nationally representative sample of U.S. children. *Environ Health* 14, 44. doi:10.1186/s12940-015-0030-y
- Xue, Z., Li, X., Su, Q. et al. (2013). Effect of synthetic pyrethroid pesticide exposure during pregnancy on the growth and development of infants. *Asia Pac J Public Health* 25, Suppl 4, 72S-79S. doi:10.1177/1010539513496267
- Zhang, L. I. and Poo, M. M. (2001). Electrical activity and development of neural circuits. *Nat Neurosci* 4, Suppl, 1207-1214. doi:10.1038/NN753
- Zhang, R., Zhang, H., Chen, B. et al. (2020). Fetal bovine serum attenuating perfluoroctanoic acid-inducing toxicity to multiple human cell lines via albumin binding. *J Hazard Mater* 389, 122109. doi:10.1016/j.jhazmat.2020.122109
- Zhang, Y., Xu, Y.-Y., Sun, W.-J. et al. (2016). FBS or BSA inhibits EGCG induced cell death through covalent binding and the reduction of intracellular ROS production. *Biomed Res Int* 2016, 5013409. doi:10.1155/2016/5013409

### Conflict of interest

KB, AD, and EF are shareholders of the company DNTOX, which provides DNT IVB assay services, and DH, CN, JW, and PZ have been or are currently employed by NeuCyte Inc., a company that commercially distributes the iN:glia co-culture described in this study, and all declare no potential conflicts of interest with respect to the research in this article. FB and EK have no conflict of interest to declare.

### Funding

This work was supported by the Danish Environmental Protection Agency (EPA) under grant number MST-667-00205, and the Horizon Europe project PARC (Grant Agreement No 101057014).

### Data availability

The dataset generated during and/or analyzed during the current study is available from the corresponding author upon reasonable request.